Lighting Up Materials with X-rays: Advanced XEOL/XAS Experimental Probe

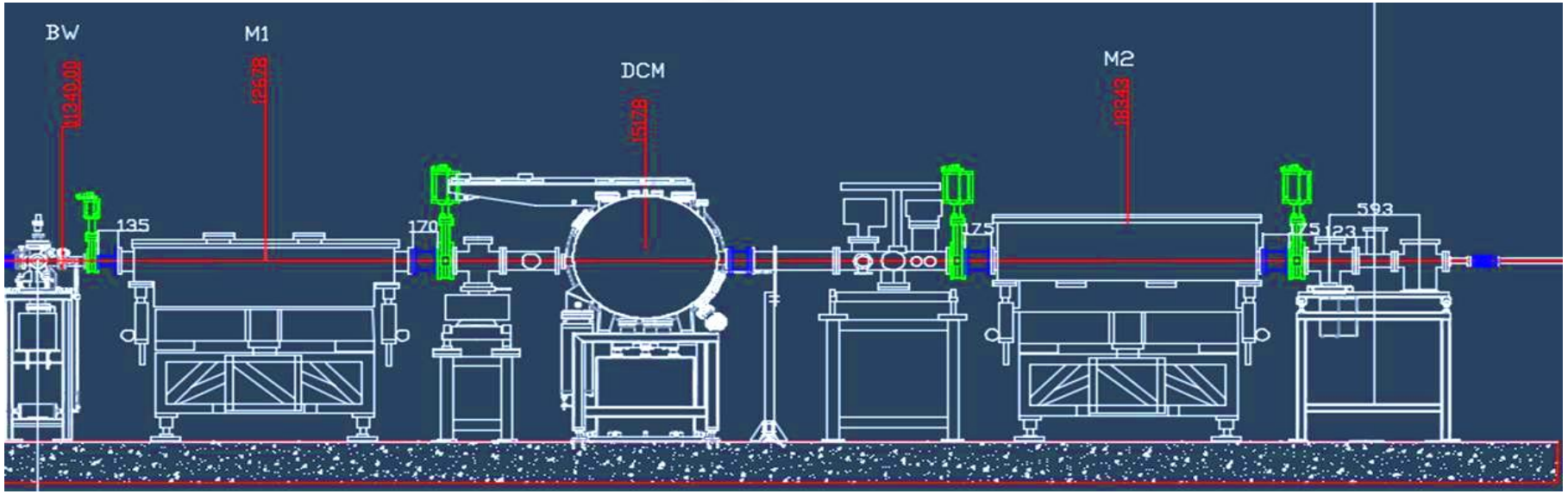

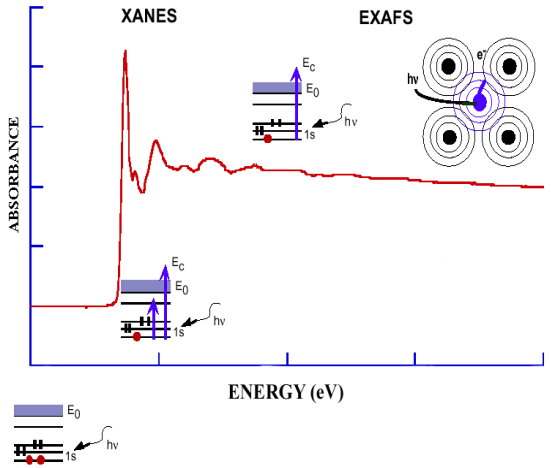

Latif Ullah Khan

Beamline Scientist

BM08-XAFS/XRF Beamline

Email: latifullah.khan@sesame.org.jo

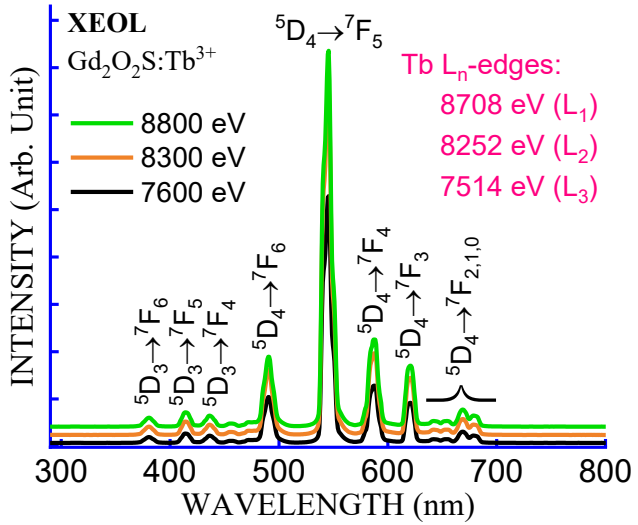

SESAME Synchrotron Light Source

World Maps
Synchrotron Light Sources

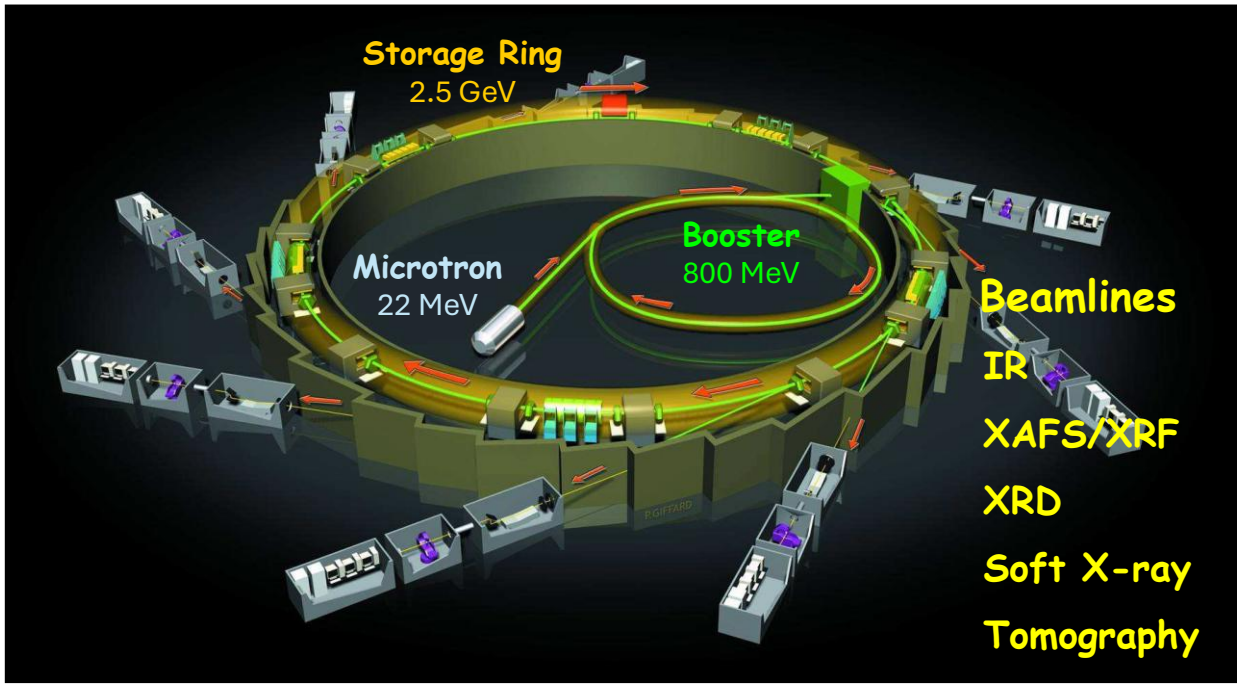

SESAME Accelerator

- Circumference: 133.2 m
- Operation current: 300 mA
- Natural emittance: 26 nmrad

❑ **There are now more than 60 synchrotrons and FELs around the world**

BM08-XAFS/XRF Beamline Optics

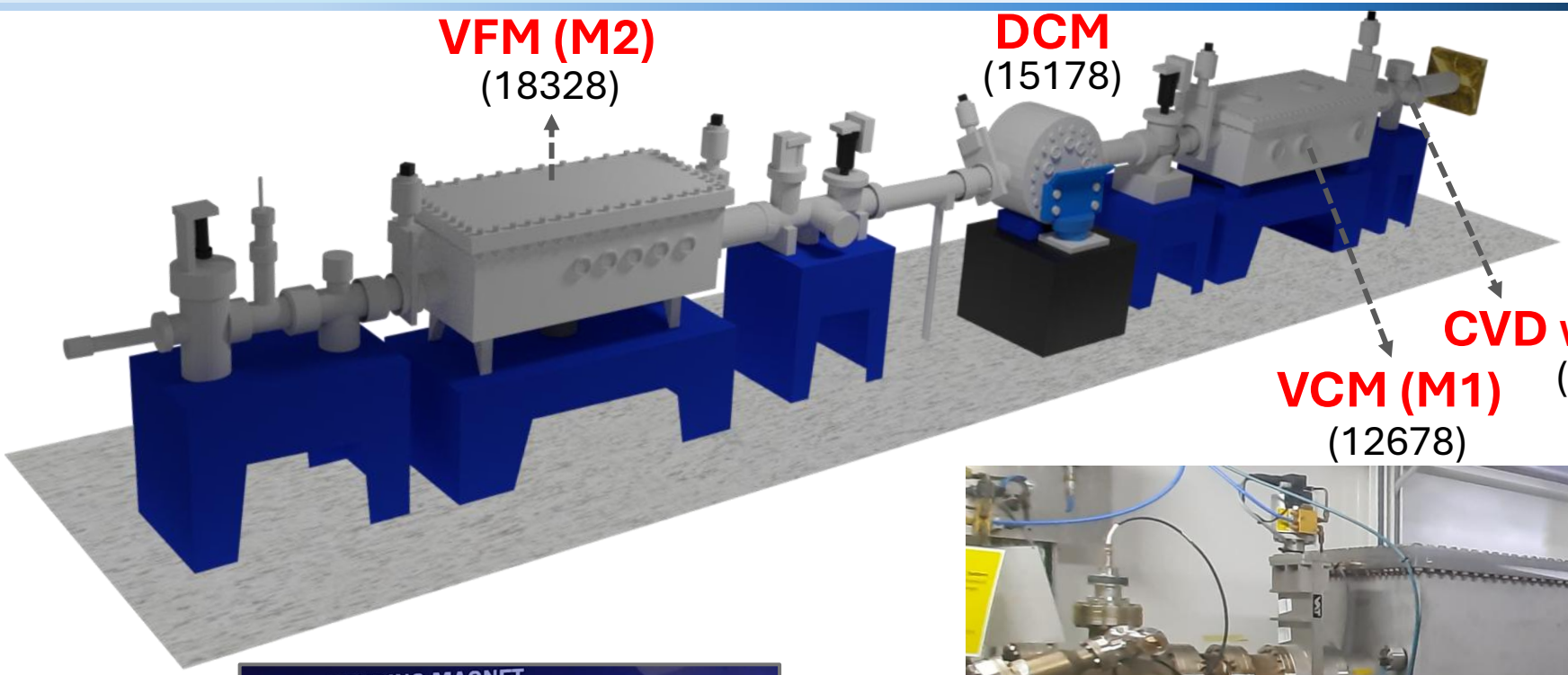

Source (D08)
Bending Magnet

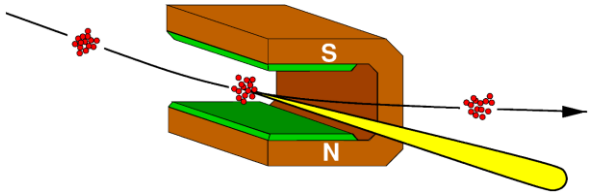

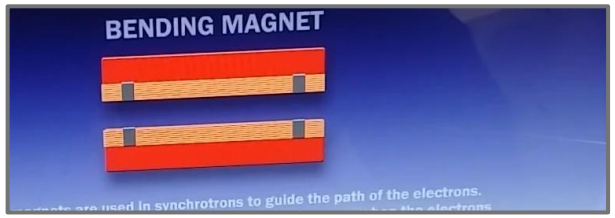

Harfouche, Khan, L.U.; Paolucci, G. et al. Emergence of the first XAFS/XRF beamline in the Middle East: providing studies of elements and their atomic/electronic structure in pluridisciplinary research fields. *J. Synchrotron Rad.* 29, 1-7, 2022.

BM08 Beamline Specifications

Parameter	Value
Magnetic field (BM)	1.4554 T
Energy Range	4.7 keV – 30 keV
Energy Resolution **Si (111)** **Si (311)**	10^{-4}
Flux	$5x10^{11}$ Ph/s @ 8 keV
Beam size (Horizontal x Vertical)	determined by slits "H x V" (max: 20 x 5 mm^2) (min: 1 x 1 mm^2)

Specifications of the Collimating and Focusing Mirrors

Specification	VCM (M1)	VFM (M2)
Dimensions (mm)	1200 x 70	1200x150
Coatings	Si, Pt	Si, Pt
Angle of incidence	Variable	Variable
Substrate	Silicon single crystal	ZERODUR
Cooling	Water cooled	Uncooled
Flatness	Cylindrical	Cylindrical
Type of bender	Pneumatic	Pneumatic
Minimum radius (km)	5.3	5.3

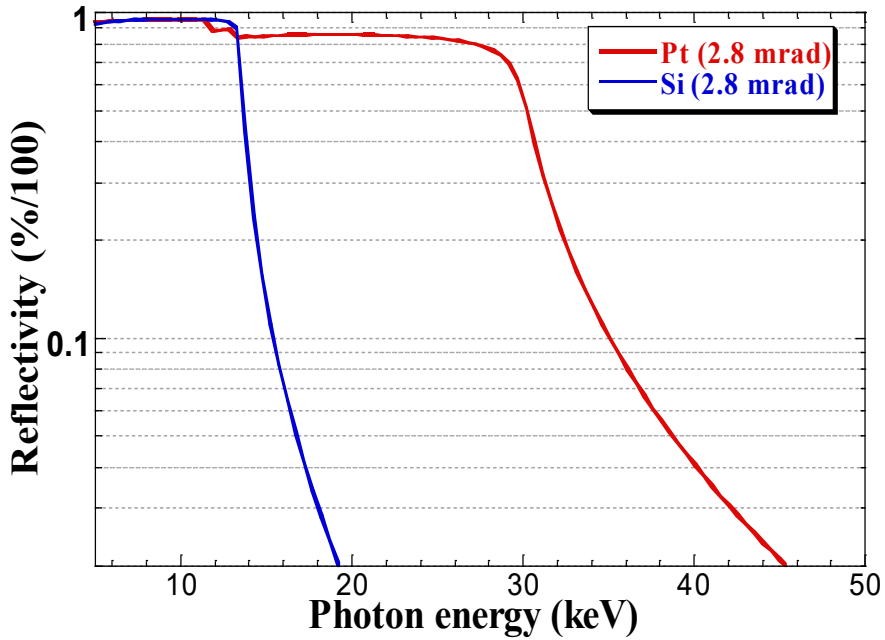

Mirrors reflectivity at 2.8 *mrad* incident beam angle for Pt and Si coatings

BM08 End Station

BM-08 XAFS/XRF Experimental Station

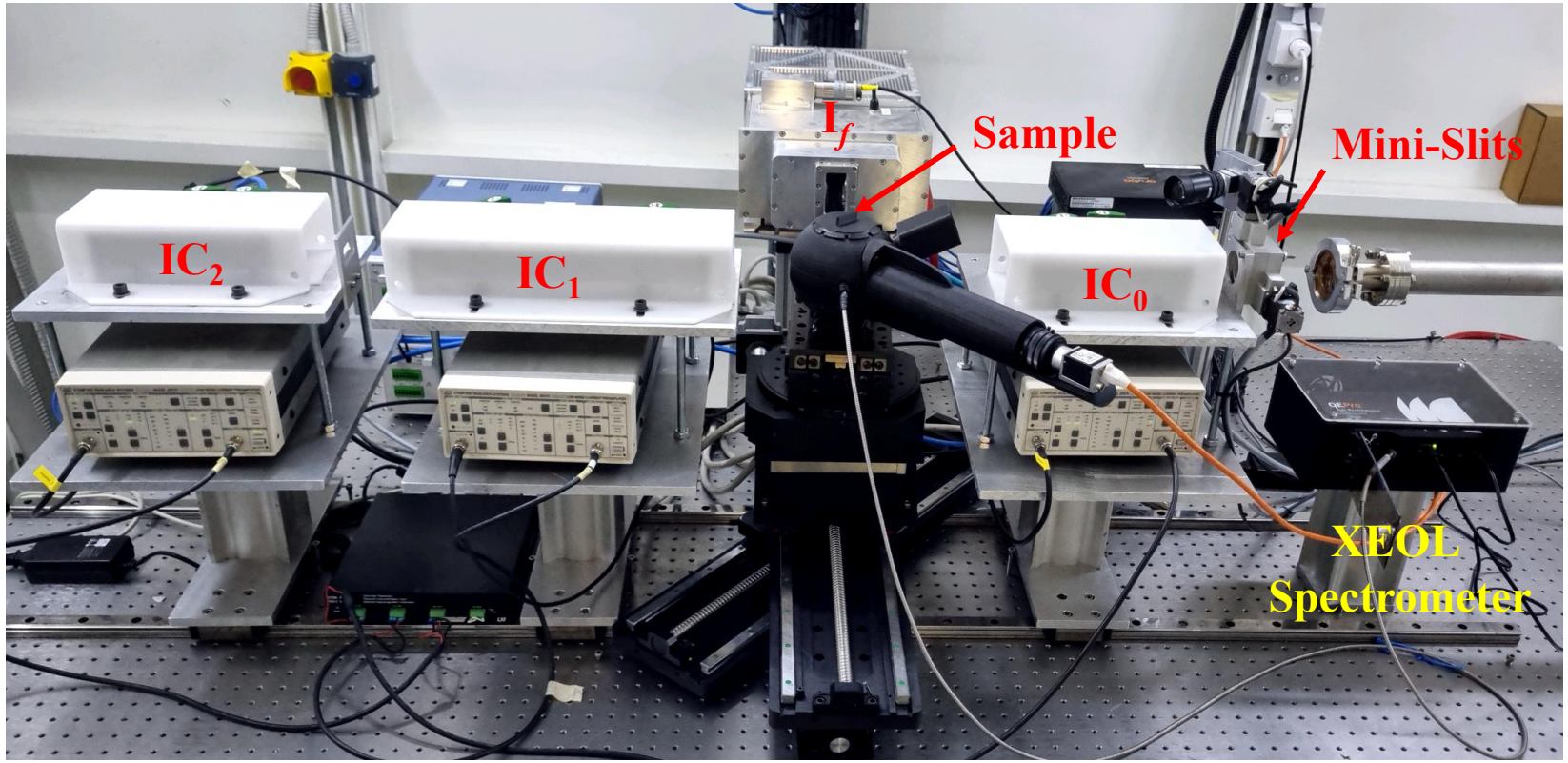

Cryojet for cooling sample (~95 K)

Techniques available

- XAFS
- XRF
- XEOL

XAFS measurement

Transmission mode: $\mu(E) = \log(I_0 / I)$

Fluorescence mode: $\mu(E) \propto I_f / I_0$

X-ray Matter Interaction

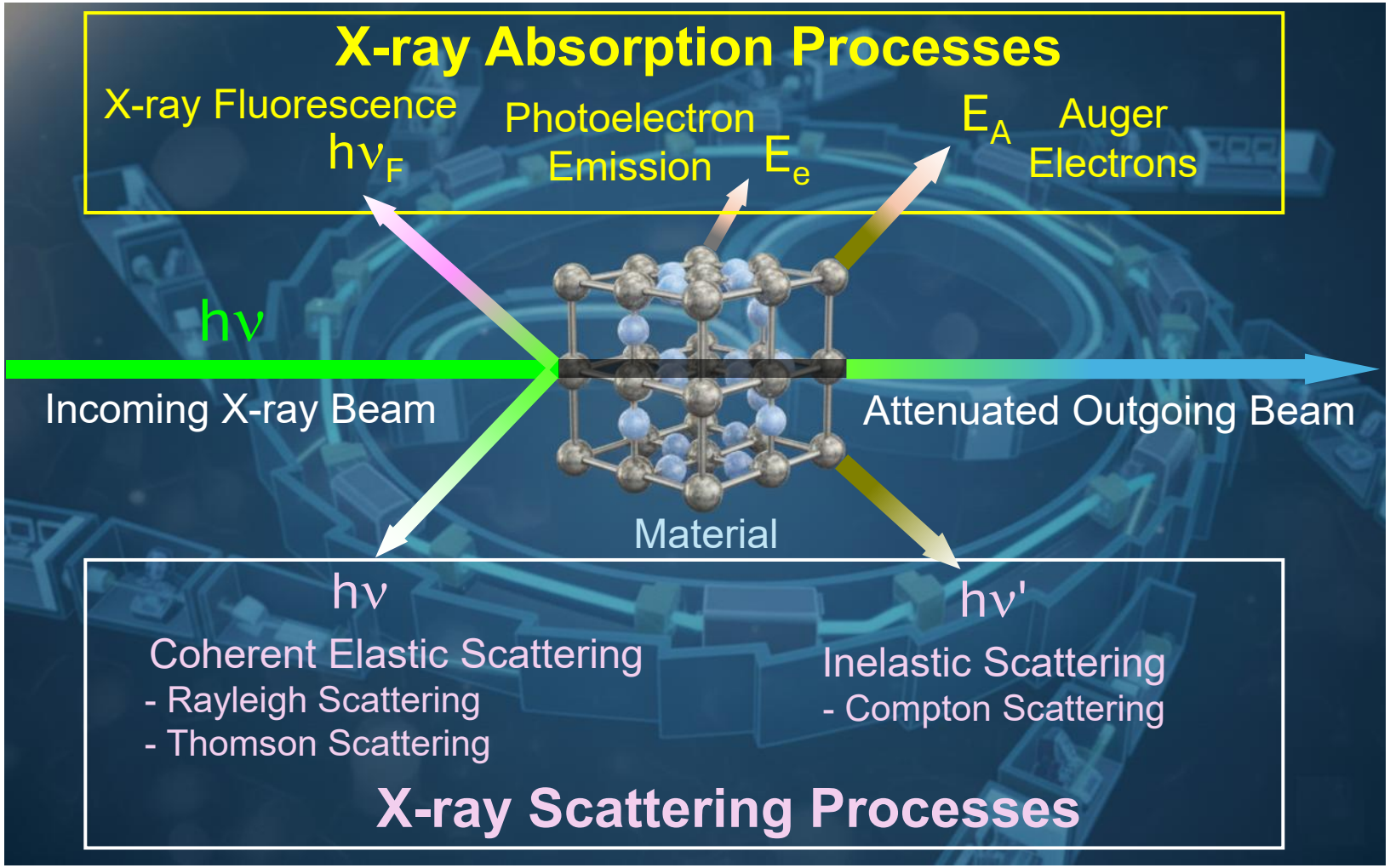

X-ray Absorption and Emission Mechanism

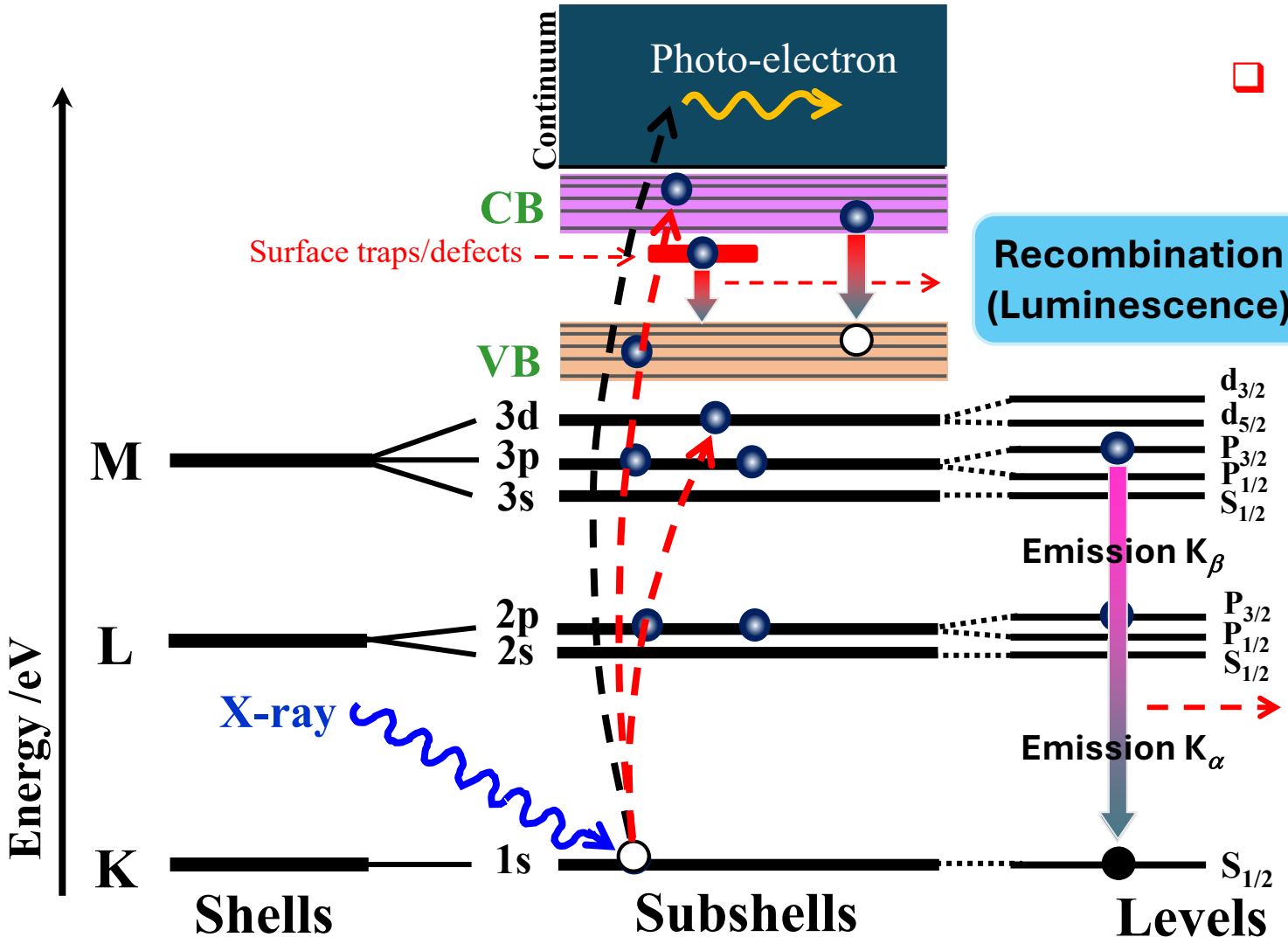

- **X-ray Excited Optical Luminescence (XEOL)**
  X-ray photon in/optical photon out technique

XEOL

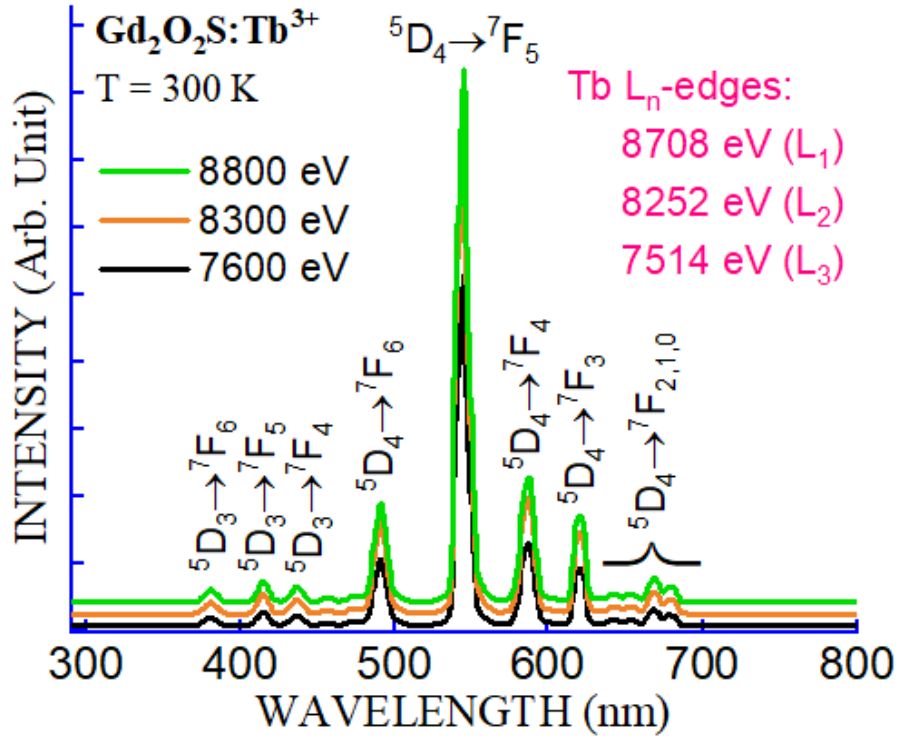

Core electron excitation by X-ray

First X-ray Absorption Spectrum

- The first X-ray absorption spectrum was observed by **Maurice de Broglie** in 1913, after a while the discovery of X-rays by Röntgen (1895). In his X-ray absorption experiment, de Broglie used X-ray tube as a source and mounted a single crystal on the cylinder of a recording barometer, employing a clockwork mechanism to rotate the crystal around its vertical axis at a constant angular speed. As the crystal was rotated, the X-rays scattered at all angles between the incident beam and the diffraction planes, according to the Bragg law, and consequently change the X-ray energy E:

$$2d_{hkl} \sin\theta = \lambda = hc/E$$

c: Speed of light (c = 2.9979 10^{+8} m/s)
h: Planck constant (h = 6.626 × 10^{-34} J s)
Thus, hc = 12.3984 Å keV

- He recorded the X-rays of varying intensities on a photographic plate and observed two distinct discontinuities on the film, proving to be the K-edge absorption spectra of silver and bromine atoms present in photographic emulsion.
- This experiment provided a foundation for the modern monochromatic beam (Monochromator)

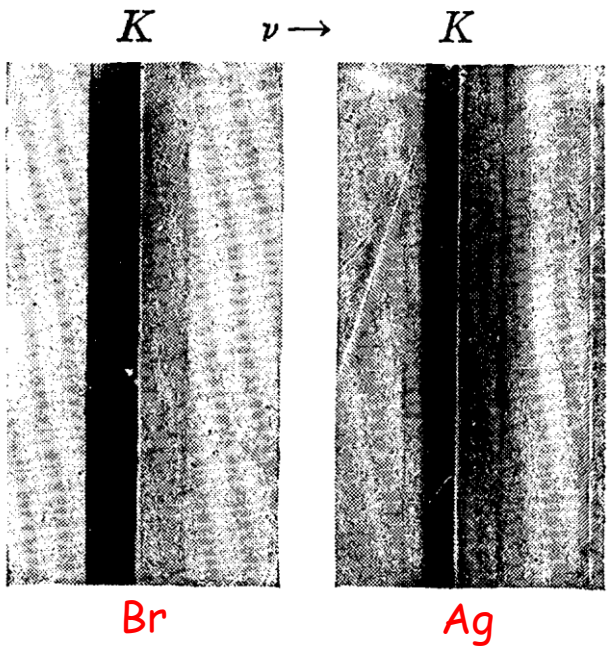

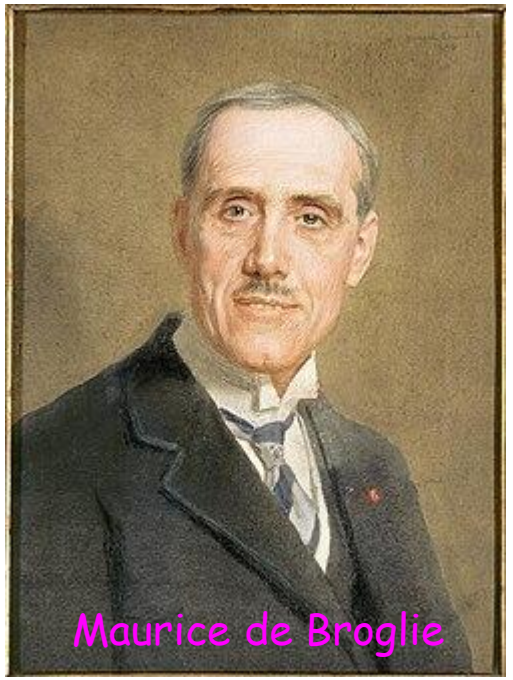

Jeroen A. Van Bokhoven and Carlo Lamberti, X-Ray Absorption and X-Ray Emission Spectroscopy: Theory and Applications. Wiley Online Lib. 2016.

J. D. Hanawalt, The Dependence of X-ray Absorption Spectra upon Chemical and Physical State. *Phys. Rev.* 1931, *37*, 715.

X-ray Absorption Spectroscopy

- There is no sharp boundary between XANES and EXAFS, so choosing an energy of demarcation is somewhat arbitrary.
- The IUCr Dictionary suggests around 50 eV above Eo (IUCr 2011), but 30 eV above Eo is also commonly used.

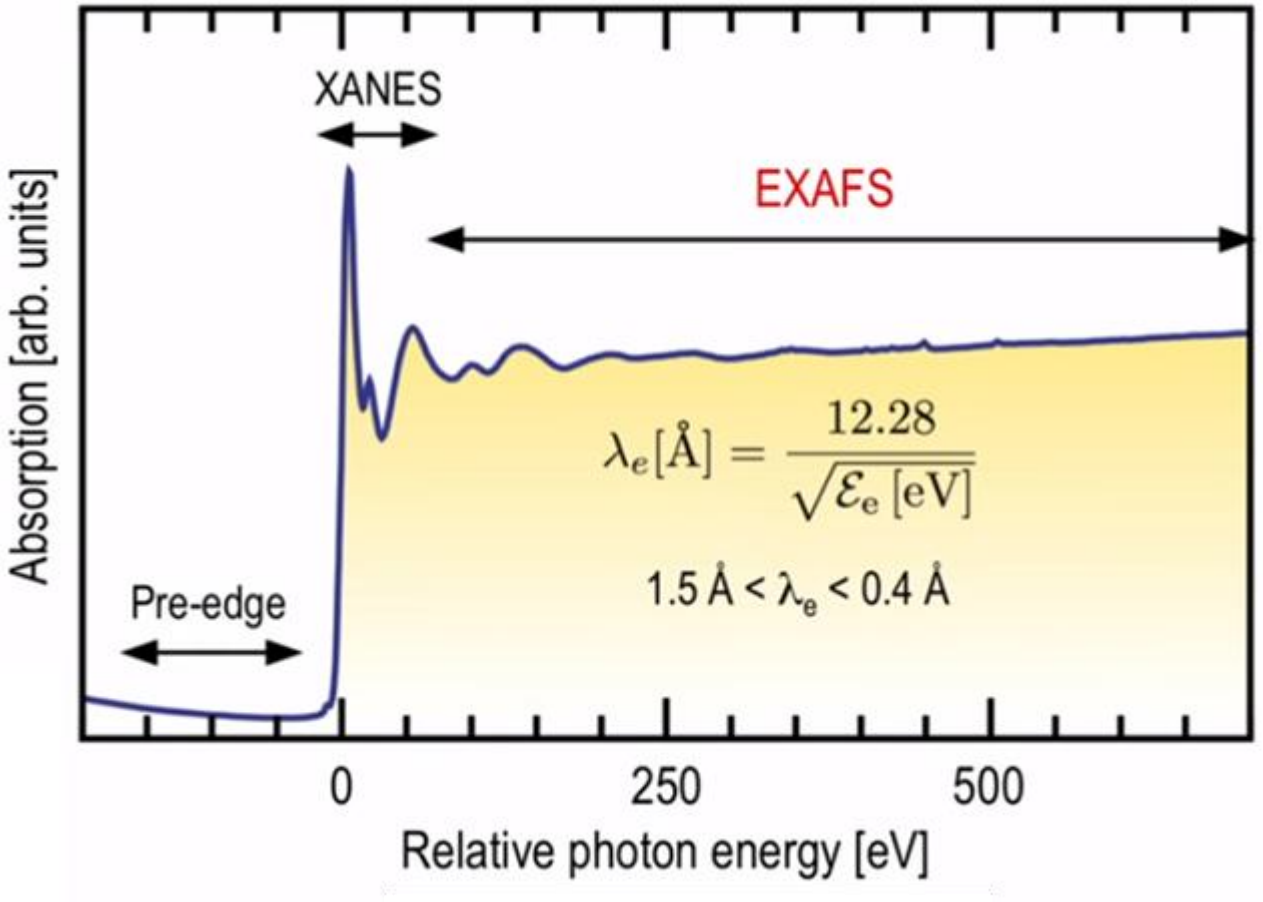

$$E = hf = \hbar\omega$$

$$p = \frac{h}{\lambda} = \hbar k$$

De Broglie

Eo is "necessary to remove the photoelectron from the atom." **Take care, it can not be always the Edge Energy**!!

XEOL Experimental Setup

BM08-XAFS/XRF Experimental Station

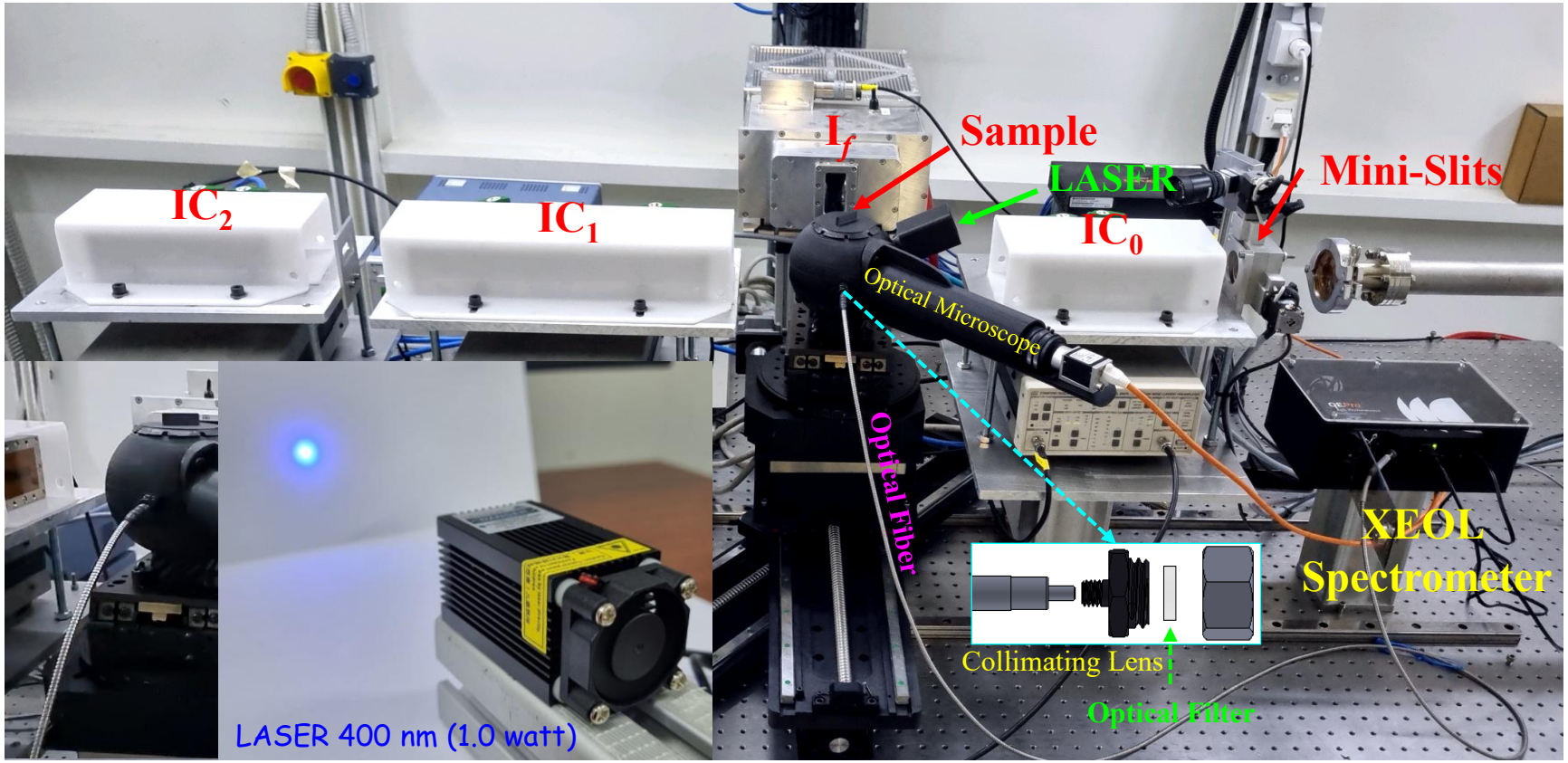

- QE Pro-ABS high-sensitivity spectrometer (Hamamatsu scientific grade back-thinned thermal electrical cooled 1024 x 58 elements CCD array detector)
- Solarization resistant optical fiber, 600 μm core diameter (0.22 NA and 200–1100 nm)
- Collimating lens (0.22 NA and 200-2000 nm)
- Basler ace GigE camera and focusing lens (40 mm focal length)

- X-ray Excited Optical Luminescence (XEOL): Spectra & Mapping
- Photoluminescence (λ: 200 – 920 nm)

Project Gant 2023: IAEA International Atomic Energy Agency

Integration of XEOL / 2D Mapping

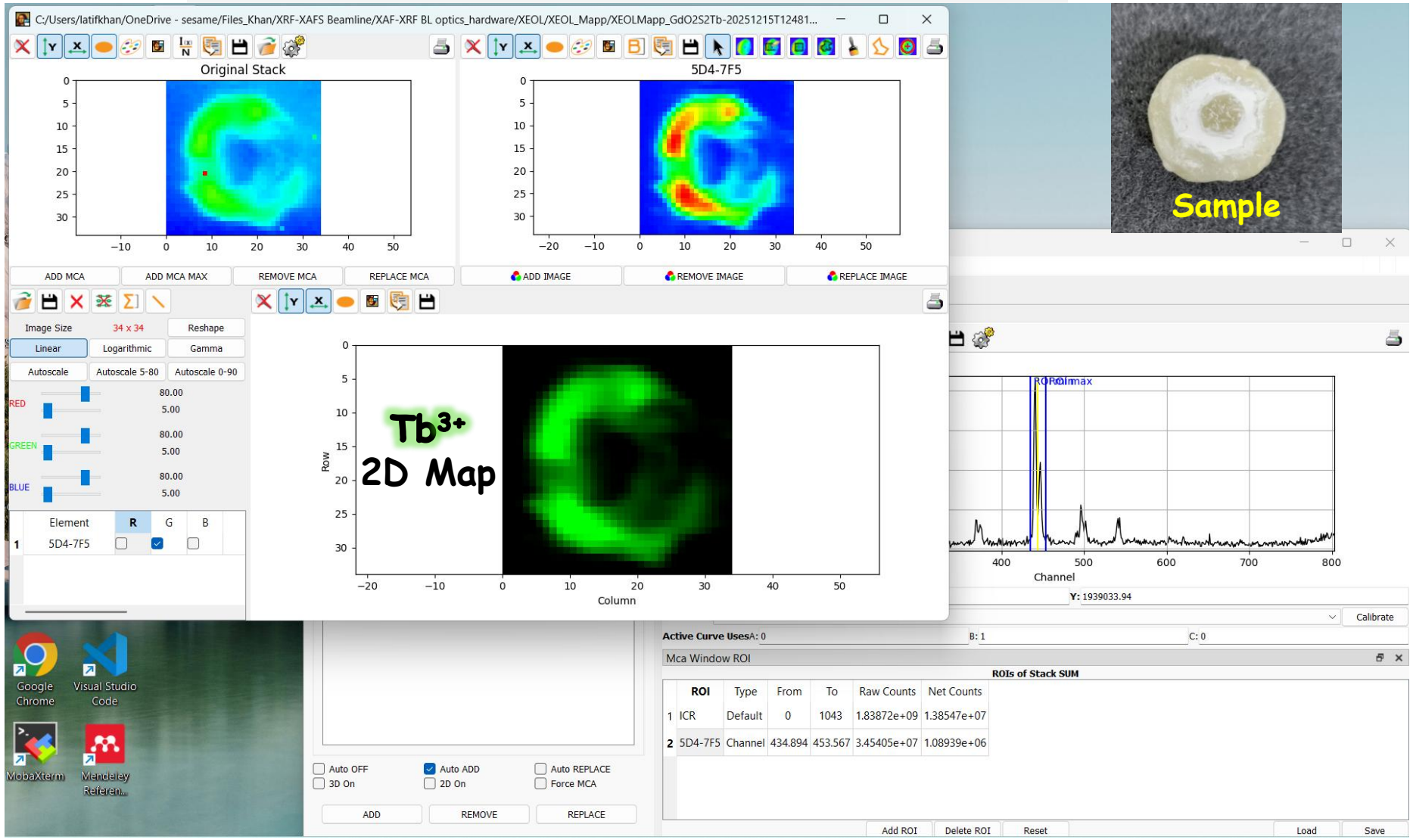

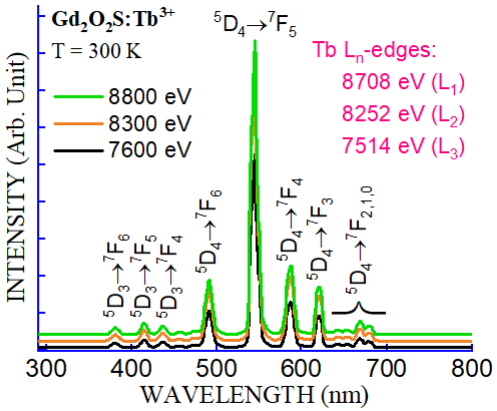

10 x 10 mm XEOL Mapping

X-ray Beam:
9000 eV

Step Size:
200 μm

Spatial Resolution:
Beam was slit down to extent that it was disappearing after closing slit by 100 μm

Rare Earths: Importance of XEOL

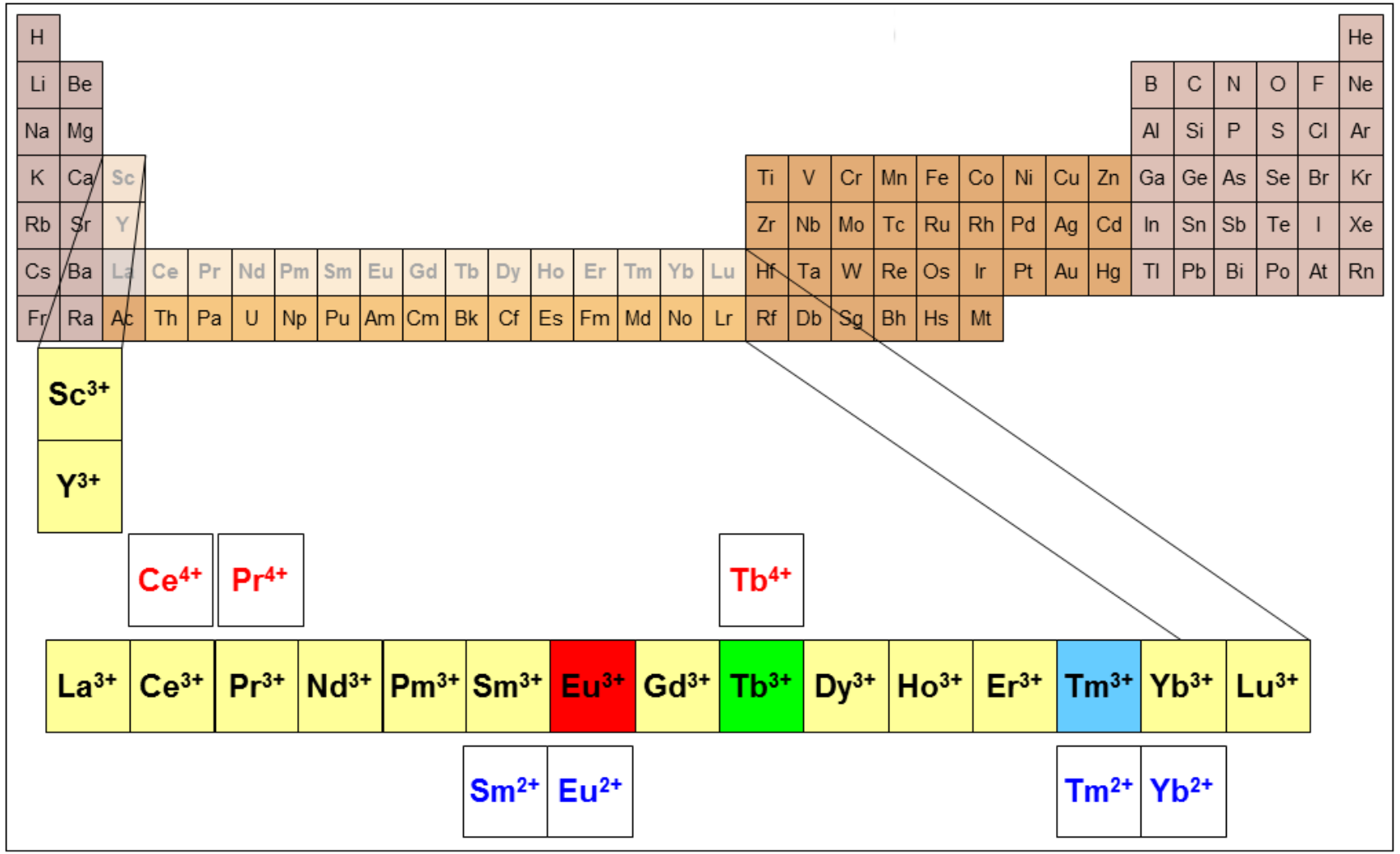

Tm – least abundant of the RE (0.5 ppm) → **It is more abundant than Cd, Ag, Pt, Au, Se…**

Global Rare Earths Reserves

- World total reserves (rounded about): 130,000,000 metric tons (130 million metric tons)
- China: 44,000,000 tons or 44 million metric tons (35%)

REEs Countries	Reserves (metric tons)
China	44000000
Vietnam	22000000
Brazil	21000000
Russia	21000000
India	6900000
Australia	4200000
United States	2300000
Greenland	1500000
Tanzania	890000
Canada	830000
South Africa	790000
Other Countries	280000
Total	130000000

U.S. Geological Survey, 2023. Mineral commodity summaries 2023. U.S. Geological Survey, 210 p.

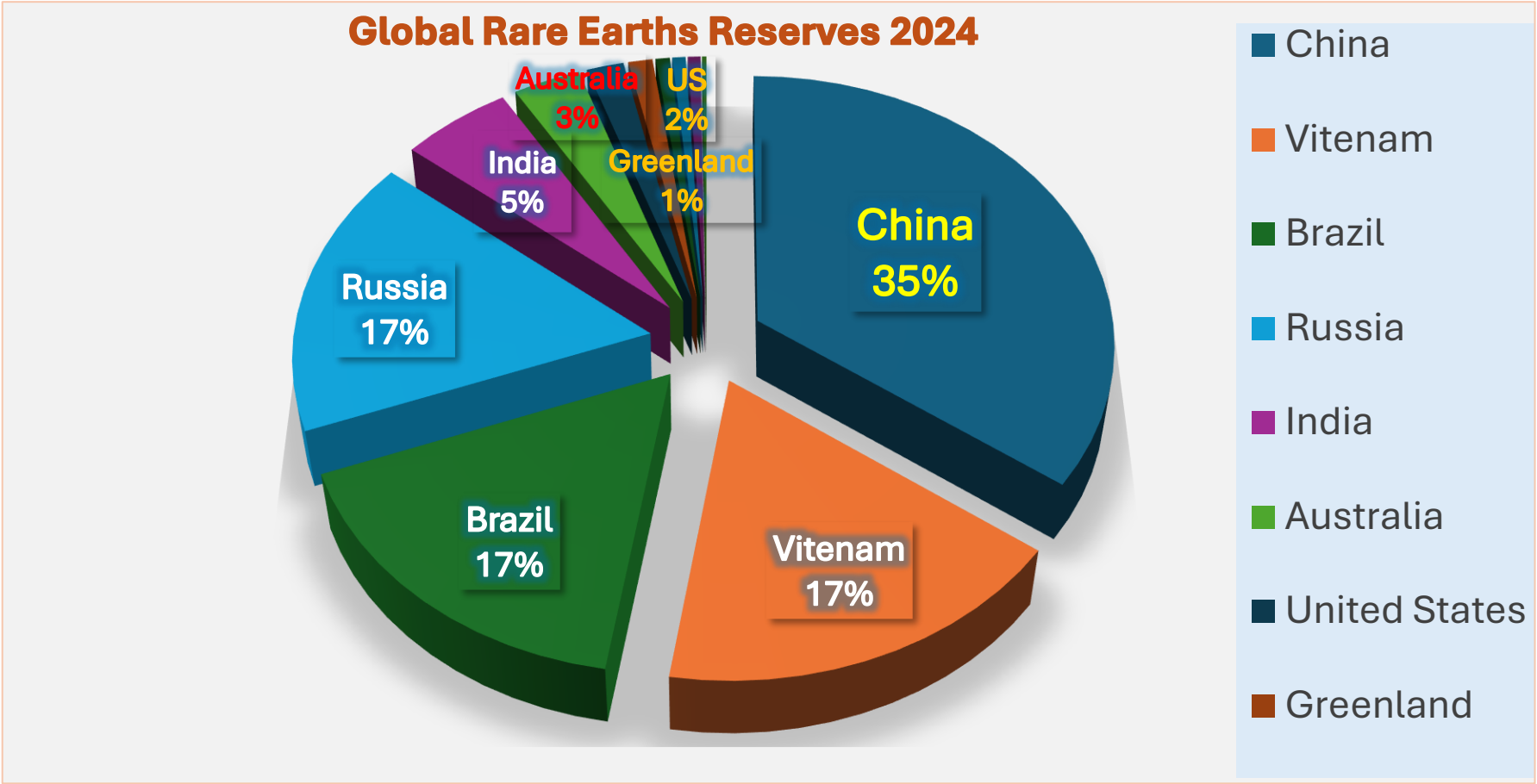

Rare Earths: Technological Applications

SESAME

Aplicacations of Phosphors

Lighting and Display
97% volume (9500T)

Y 69,6% Ce 10,9% La 8,3%
Eu 4,9% Tb 4,5% Gd 1,8%

Medical Other Laser

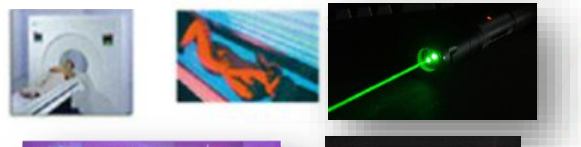

Optical Markers

Persistant luminescent

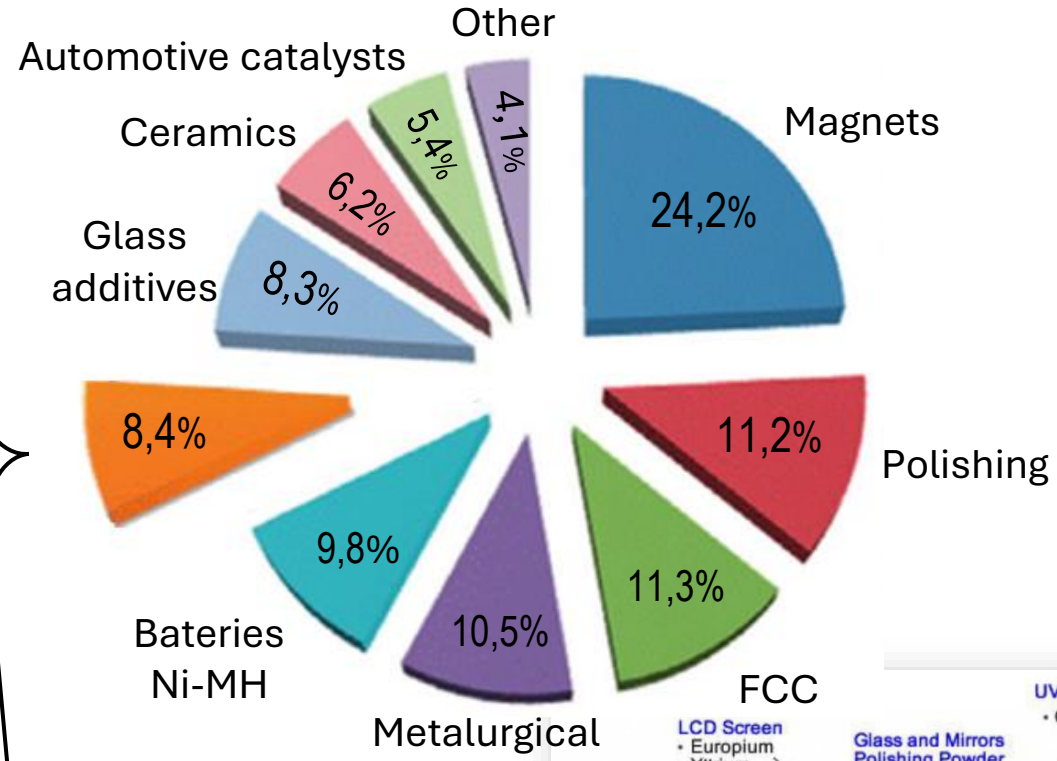

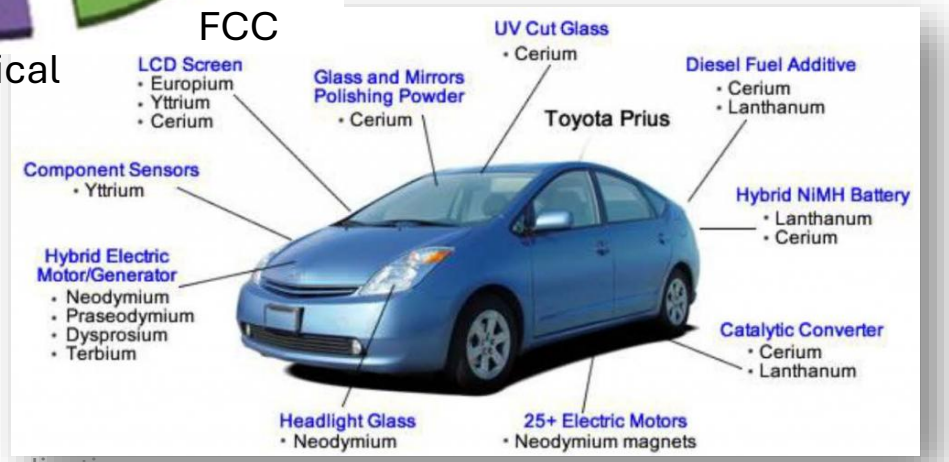

J. Lucas, P. Lucas, T. Le Mercier, A. Rollat, W. Davenport, in:, Rare Earths, Elsevier, 2015

RE^{3+} Energy Levels: 4-10 eV Energy Range

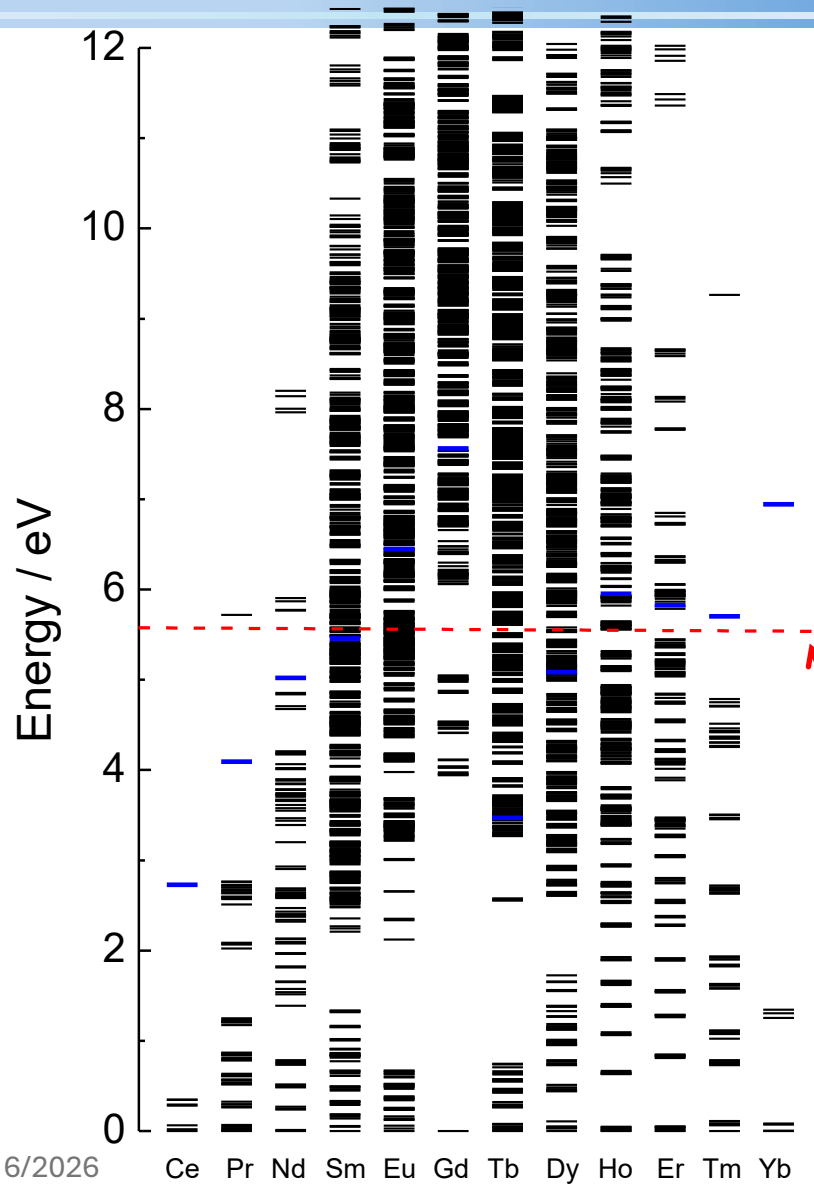

Energy range 4-10 eV needed for:

- Host band gap energy (E_g) determination
  - Essential for *e.g.* persistent luminescence materials
    - Example: 7.1 eV for $Sr_2MgSi_2O_7:Eu^{2+},Dy^{3+}$
- Study of dopant energy levels structure in the **VUV** range (> 6 eV)
  - High 4f levels and 5d levels.
    - Quantum cutting materials (*e.g.* $KMgF_3:Pr^{3+}$)
- Higher photon flux needed than with lab equipment
  - High sensitivity
- Measuring fast kinetics (ns) and time resolution

- Synchrotron Radiation Source offers a high brightness, photon flux, tunable energy and temporal stability than the most sophisticated Laboratory Source.

High energy limit of laboratory set-ups: 5.6 eV

XEOL/XAS Role: RE Persistent Luminescent

- For full understanding luminescence mechanism in **solid materials** **(phsophors)**, the optoelectronic structure need to be studied:
  - Host lattice structure
  - Band gap
  - Rare earth (RE) (4f levels)
  - RE local sites in host lattice
  - RE oxidation state
  - Structural defects

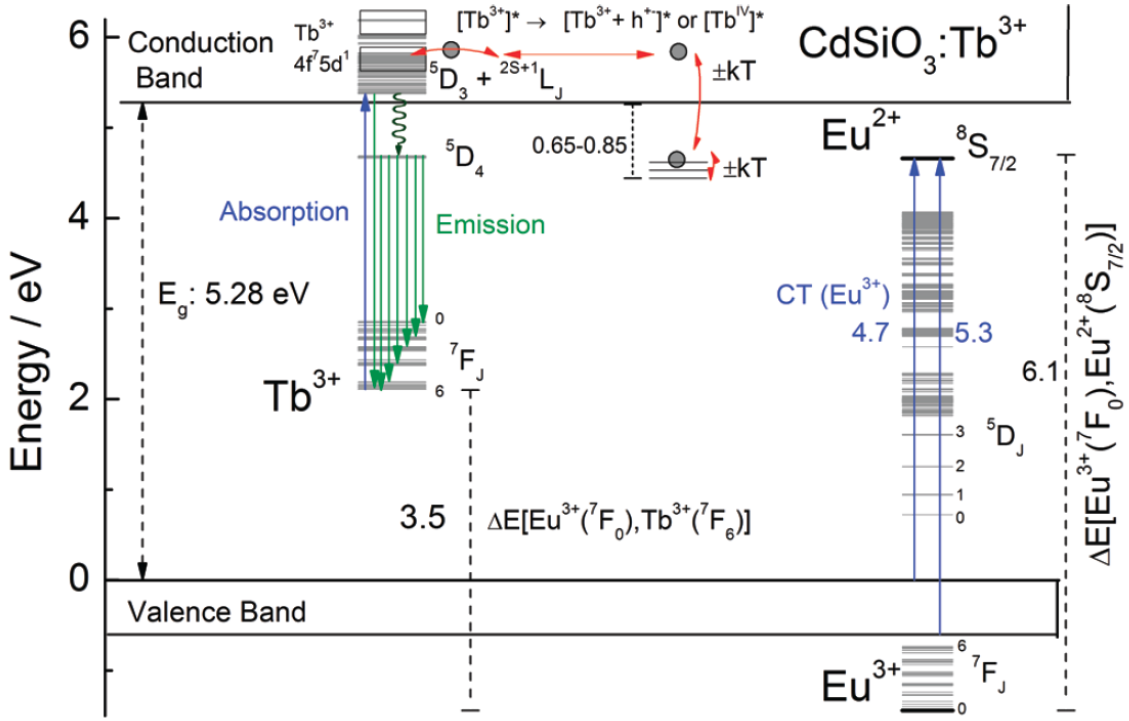

Persistent luminescence mechanism of Tb^{3+} in $CdSiO_3$ (After Glow)

- Goal: models for predicting the fundamnetal luminescence mechanism of after glow materials
  - Combining experimental and theoretical optical and spectroscopic/strcutural methods
  - Probing photormitter RE sites/oxidation sates (emission center) by XEOL/XAS

Complementary Techniques: Eu Scintillator

SESAME

- Probing Eu^{2+}/Eu^{3+} sites in $BaAl_2O_4:Eu$
- XRD / XAS / XEOL

XRD: Long range Structure

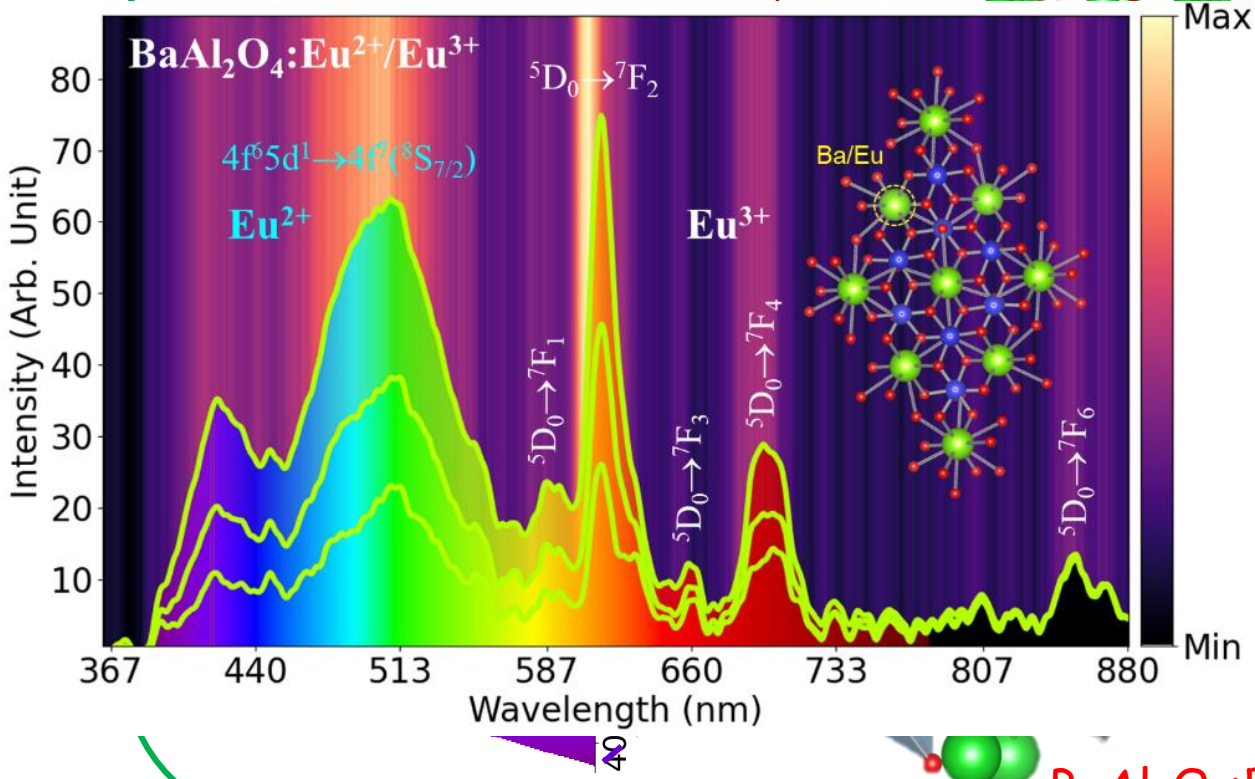

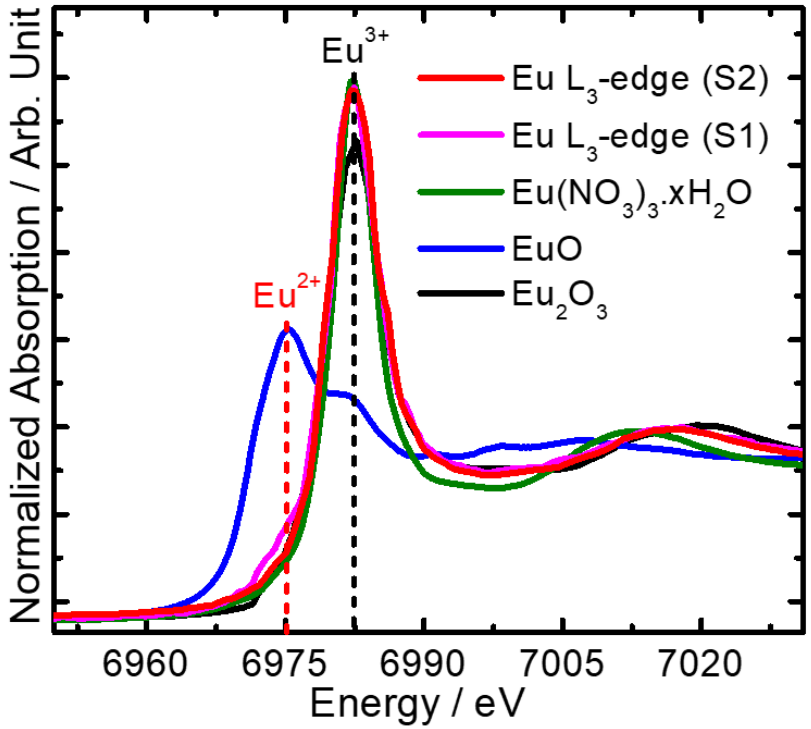

$BaAl_2O_4:Eu$

Latif U. Khan et al. Advanced Probing of Eu^{2+}/Eu^{3+} Photoemitter sites in BaAl2O4:Eu scintillators by Synchrotron Radiation X-ray Excited Optical Luminescence Probe. *Optical Materials*, 162, 116937, 2025.

THE UNIVERSITY OF JORDAN

GGG:Eu: X-ray Scintillator

SESAME

RE Scintillator in Computed Tomography (CT)

XEOL Spectrum of $Gd_3Ga_5O_{12}:Eu^{3+}$ (GGG:Eu) scintillator

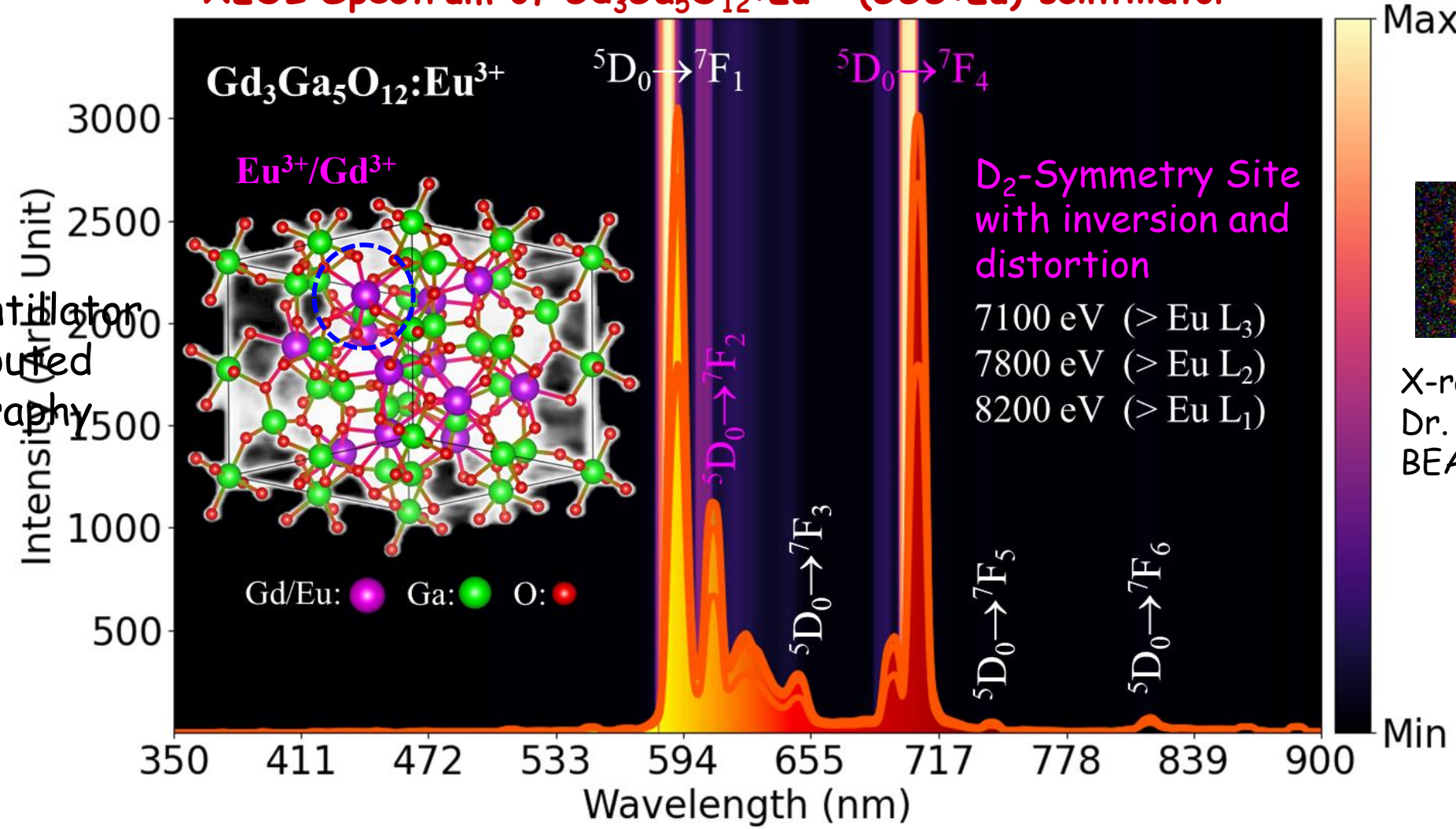

GGG:Eu

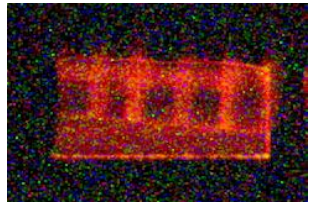

X-ray Scintillator from Dr. Fareeha Hameed BEATS Beamline

Sm Complex Scintillator

XEOL Spectrum of [Sm(dbm)3(phen)] complex (organic scintillator)

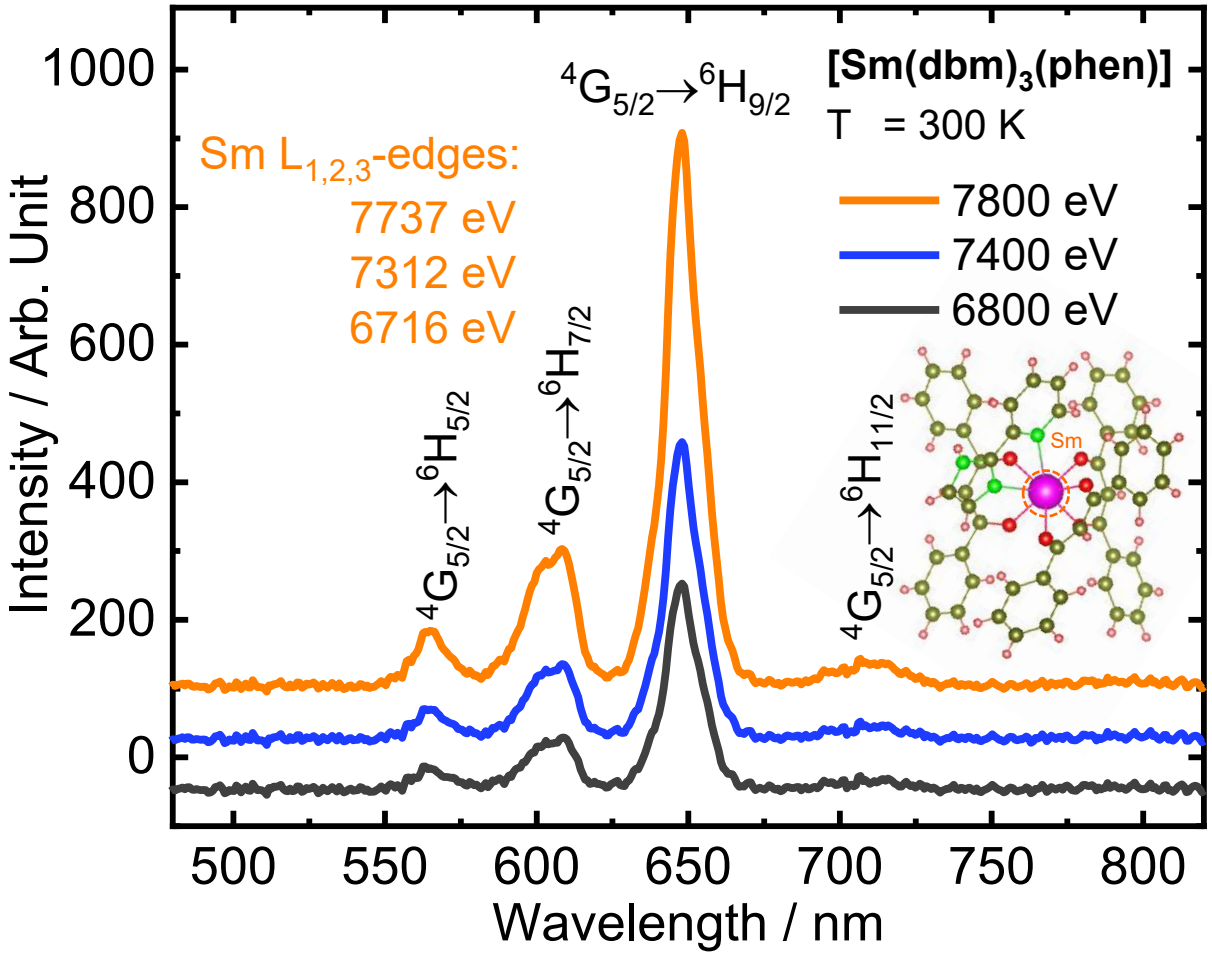

Khan, L.U. et al. Tracking coordination environment and optoelectronic structure of Eu^{3+} and Sm^{3+} sites via x-ray absorption spectroscopy and x-ray excited optical luminescence. *Materials Today: Proceedings*, 2024. https://doi.org/10.1016/j.matpr.2024.03.028

XEOL/XAS: Role of RE^{3+} in QDs Emission

XEOL Spectra:ZnSe:Mn^{2+},RE^{3+} Quantum Dots

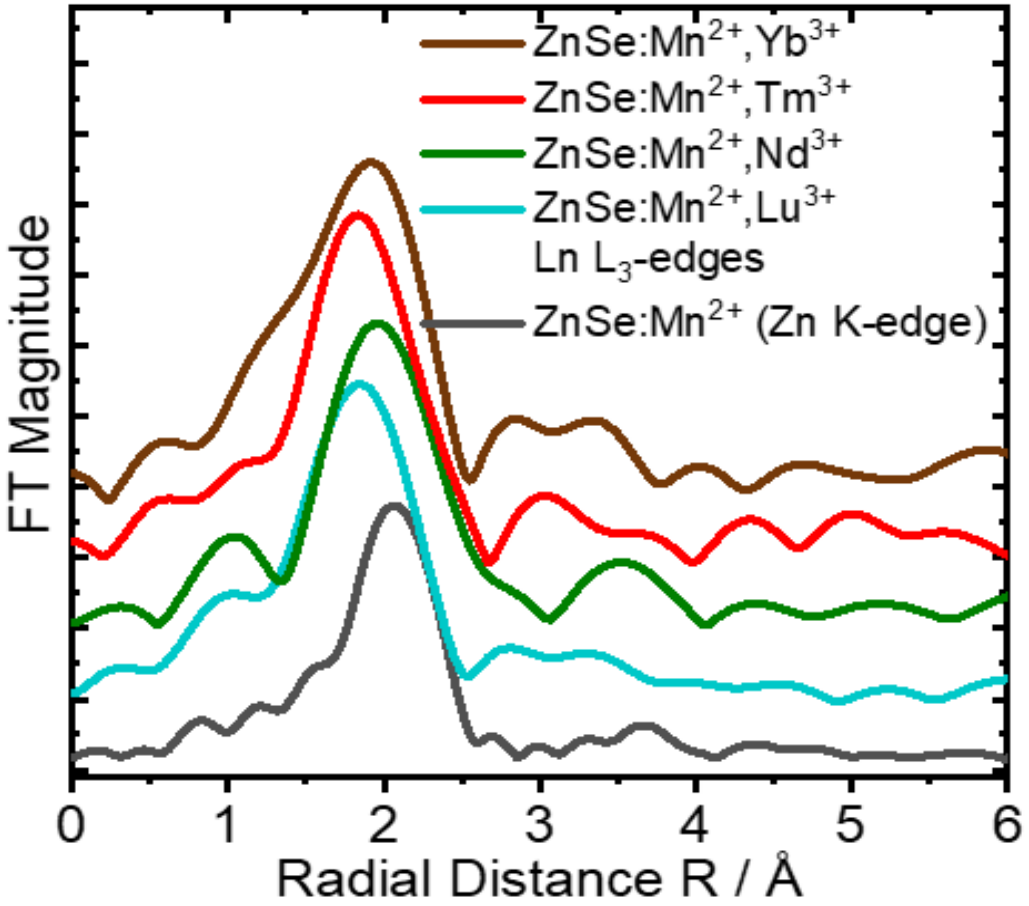

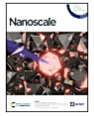

From the journal:
Nanoscale

Ln^{3+}-ion-mediated enhancement in UV/X-ray-induced optical emission from Mn^{2+}-doped ZnSe nanocrystals†

Check for updates

Iram Gul,[ab] Zahid U. Khan,[*bc] Muhammad Abdullah Khan,[a] Gabriel A. Cabrera-Pasca,[b] Ruba I. AlZubi,[d] Santiago J. A. Figueroa,[e] Hermi F. Brito[c] and Latif U. Khan[*cf]

Author affiliations

* Corresponding authors

[a] Renewable Energy Advancemnet Laboratory, Department of Environmental Sciences, Quaid-i-Azam University (QAU), Islamabad, Pakistan

[b] Research Centre for Greenhouse Gas Innovation, University of Sao Paulo (USP), São Paulo, SP, Brazil
E-mail: zahid@iq.usp.br

[c] Institute of Chemistry, University of São Paulo (USP), São Paulo, SP, Brazil
E-mail: latifkhn@iq.usp.br, latifullah.khan@sesame.org.jo

[d] Jordan Atomic Energy Commission, Amman 11934, Jordan

[e] Brazilian Synchrotron Light Laboratory (LNLS), Brazilian Center for Research in Energy and Materials (CNPEM), Campinas, São Paulo, Brazil

[f] Synchrotron-light for Experimental Science and Applications in the Middle East (SESAME), P.O. Box 7, Allan 19252, Jordan

Gul, I.; Khan, Z.U.; Khan, L.U. et al. Ln^{3+} Ions-Mediated Enhancement in UV/Xray Induced Optical Emission from Mn^{2+} doped ZnSe Nanocrystals. *Nanoscale (RSC),* 17, 15393-15401, 2025

ET in UCNPs: Tm^{3+}/Mn^{2+} Emission

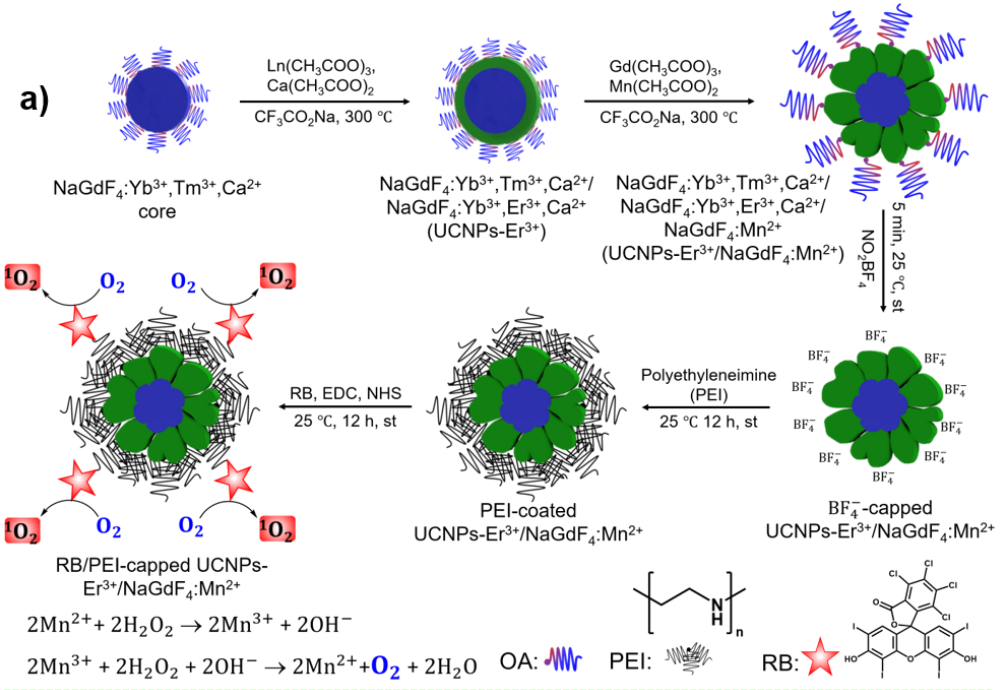

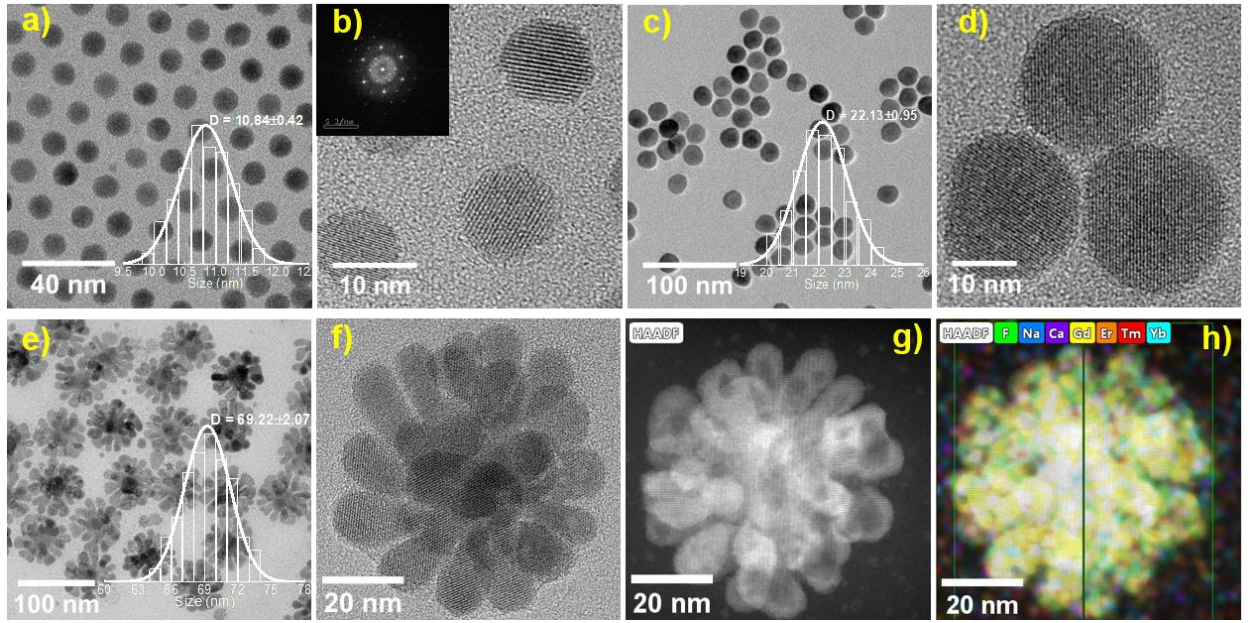

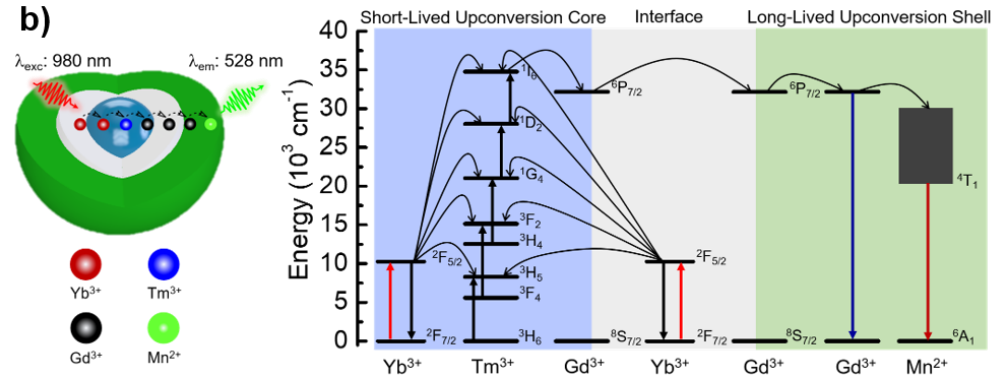

- Energy migration mechanism among the RE^{3+} and Mn^{2+} ions dopants in core/shell lattices of UCNPs.
- Short-lived Tm^{3+} blue emission and long-lived Mn^{2+} green emission under irradiation with 980 nm.

Khan, Z.U. et al. Manipulation of Energy Migration in Upconversion Nanoparticles for Long-Lived Mn^{2+} Emission and Enhanced Singlet Molecular Oxygen Generation. ACS Appl. Nano Mater. 7, 21104–21113, 2024.

Energy Materials: RE in Solid Oxide Fuel Cell

SESAME

Zahid Ullah Khan (PhD)

Research Center for Greenhouse Gas Innovation
Engineering School, University of São Paulo

Cath
(LaSrC

Electrolyte (8YSZ)

LCF: 77 % Ni metal and 23% NiO

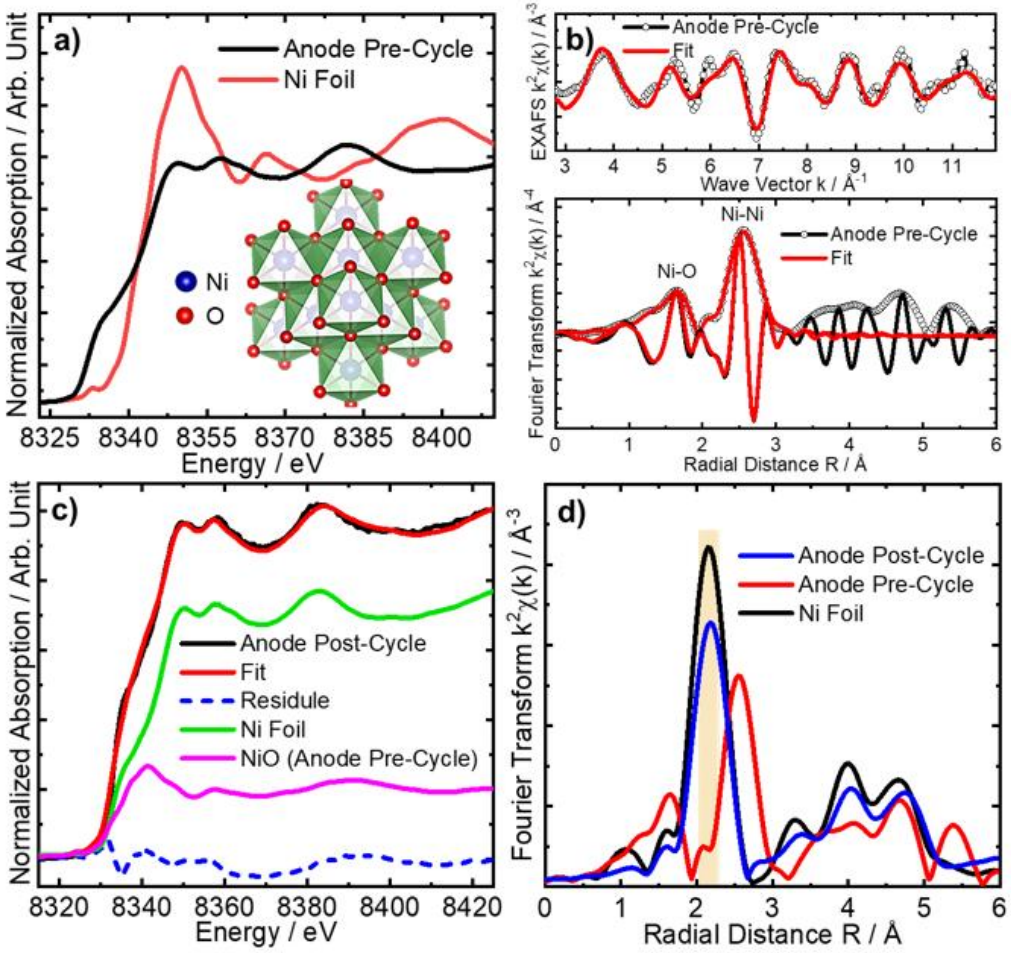

Gabriel A. Cabrera-Pasca, Zahid U. Khan et al. Unrevealing the Electrochemical Performance and Limitations of Anode-Supported 2R-Cell™ SOFC *via* Synchrotron Radiation XAFS and Impedance Spectroscopy Journal of Power Sources (ELS) under revision 2026.

Catalysis / Electrocatalysis: EXAFS Simulation

- Nickel ion-implanted Coblat (II) Oxides thin films deposited on the Fluorine-doped Tin Oxide (FTO) glass (Fixed fluence: 1×10^{15} cm^{-2}), using Pelletron Tandem Accelerator (Energy: 700 KeV).

Energy: 700 keV-35 MeV
Beam spot: 0.5 to 8 mm

Ion beams : H, He, B, P, C, Si, P, Ni, Cu, Fe, Au

- Exploring point defects/oxygen vacancies in these samples *via* XRD and XAFS to enhance their efficiencies for application as electrocatalysts in Hydrogen Evolution Reaction - HER (Fuel Cells).

EXAFS Simulation by Evolutionary Algorithm Implemented in Reverse Monte Carlo method (EA-RMC) – EvAX code.

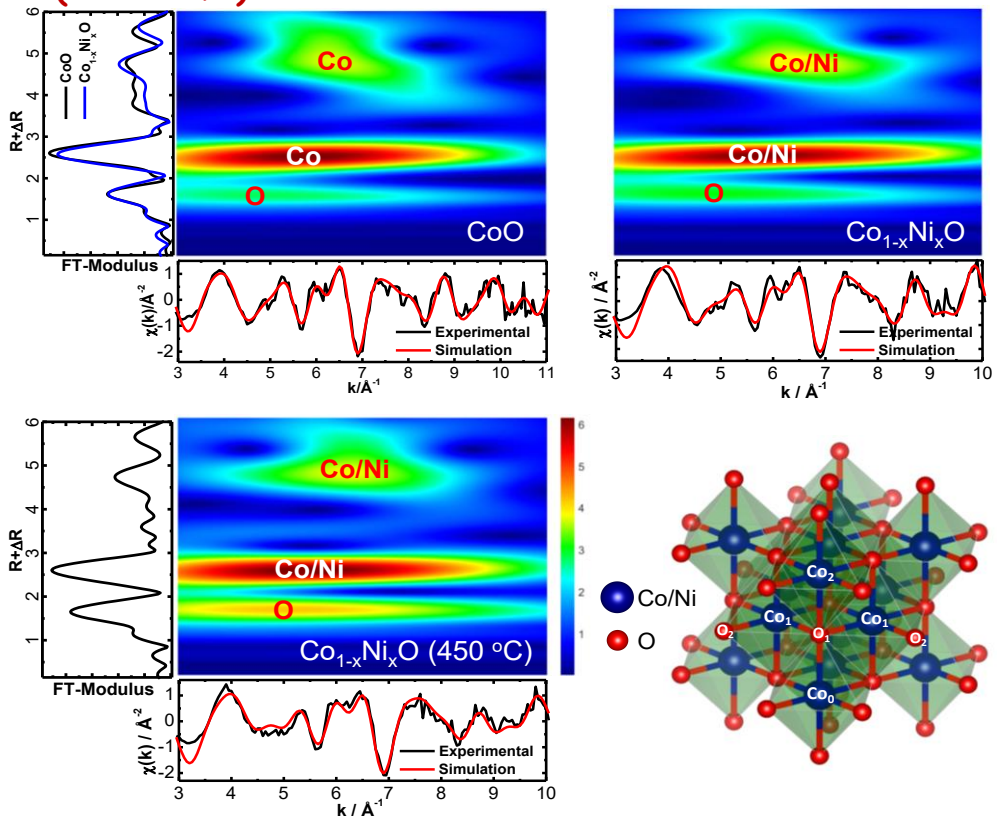

Muhammad Usman, Sibgha Sajid, Latif U Khan, et al. Defect engineering in ZnO Nanorods via phosphorous ion implantation and post-annealing recovery. Journal of Alloys and Compounds, 184075, **2025**. https://doi.org/10.1016/j.jallcom.2025.184075

Latif U Khan, Naila Jabeen et al. Investigating Local Structure of Ion-Implanted (Ni^{2+}) and Thermally Annealed Rocksalt CoO film by EXAFS Simulation Using Evolutionary Algorithm. *ACS Applied Energy Materials (ACS) 4,* 2049–2055, **2021**. https://doi.org/10.1021/acsaem.0c02676

Emission Color-Tunable CdSe/ZnS

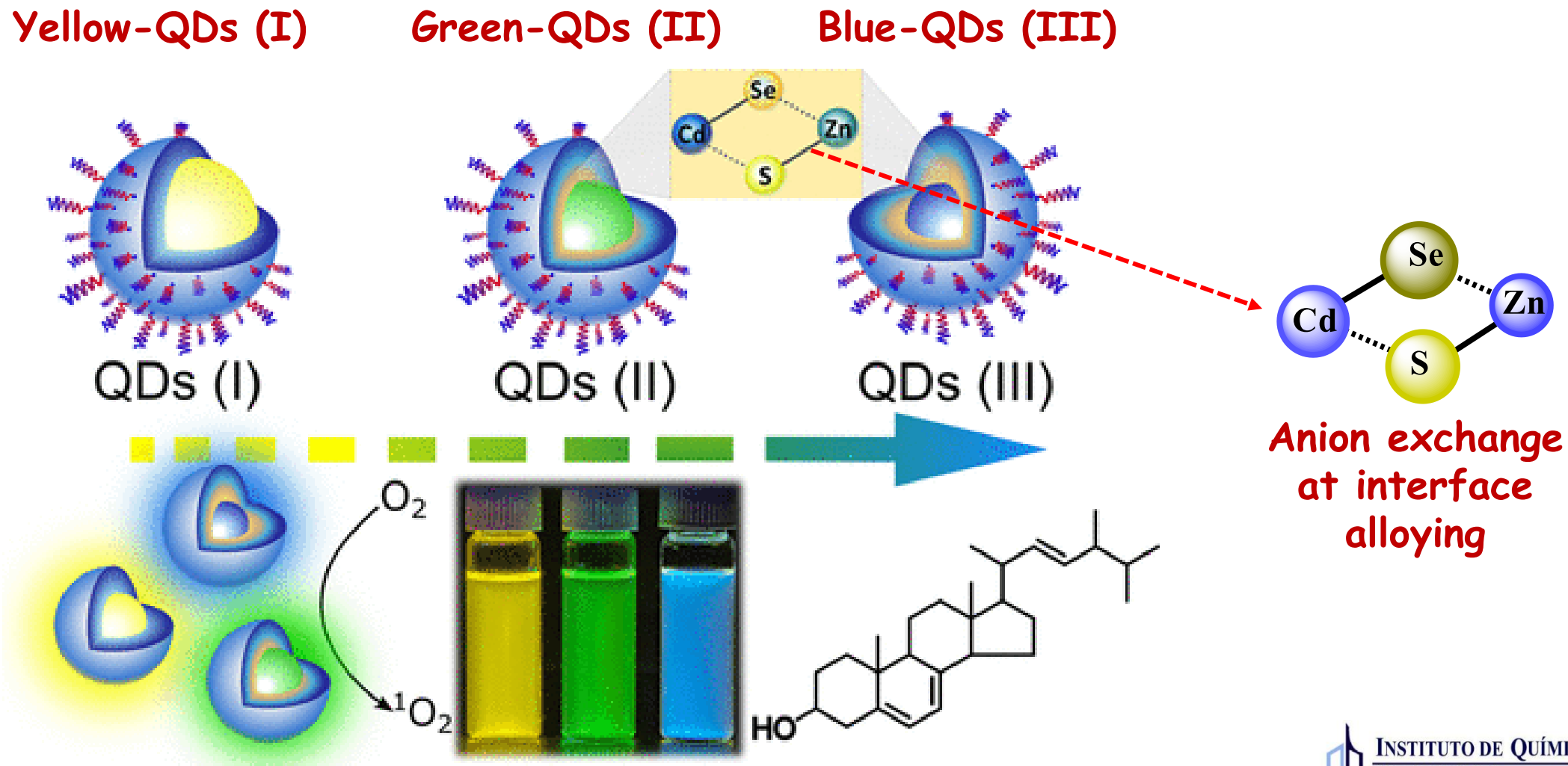

Khan, Z.U.; Khan, L.U. et al. Singlet Molecular Oxygen Generation *via* Unexpected Emission Color-Tunable CdSe/ZnS Nanocrystals for Applications in Photodynamic Therapy. *ACS Appl. Nano Mater.* 6, 3767–3780, 2023

Probing Anion Exchange in CdSe/ZnS - XAFS

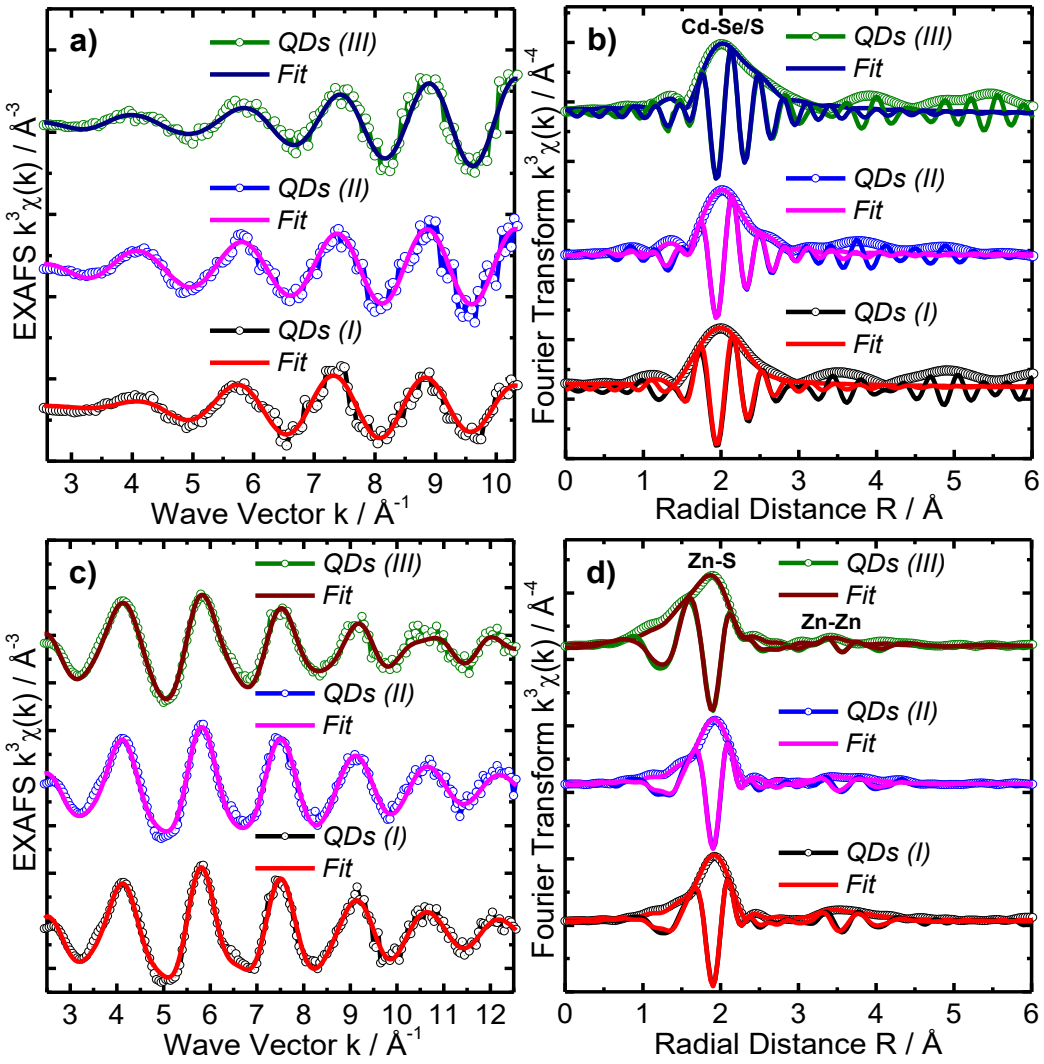

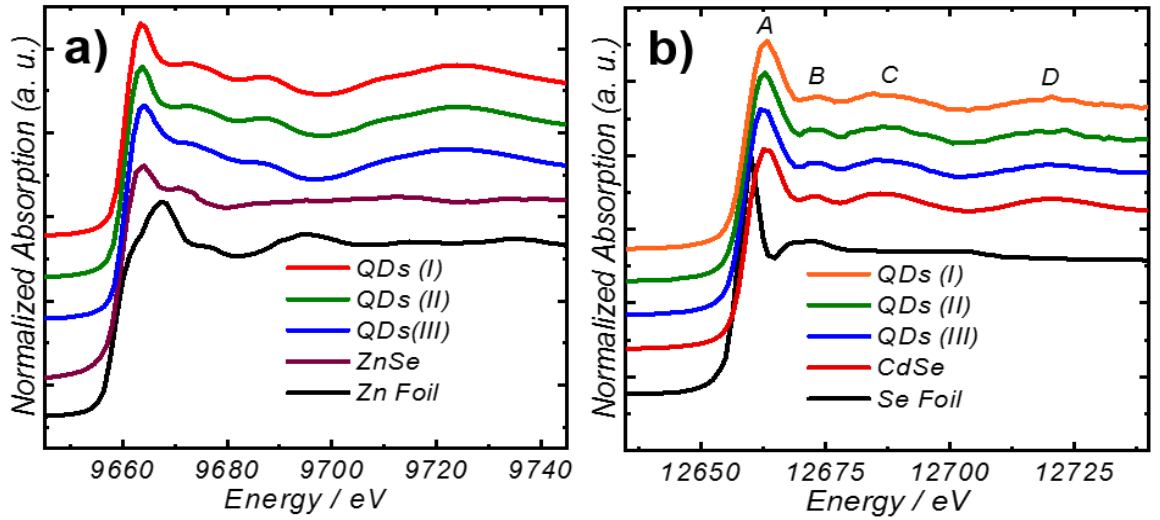

Table 1. Derived EXAFS fitting parameters, including N: number of neighboring atoms, R: distance between absorbing atom and its neighbors, σ^2: mean square relative displacements (MSRDs) or Debye–Waller factor, S^0_2: amplitude reduction factor and R_{factor}: goodness of fit for the QDs **(I)**, QDs **(II)**, and QDs **(III)**.

Material	Bond Type	N	R(Å)	σ^2(Å^2)	S_0^2	R_{factor}
QDs (I)	Cd-Se	4	2.531±0.008	0.01048±0.00088	1.0	0.0210
QDs (II)	Cd-S	2	2.494±0.009	0.00189±0.00055	0.9	0.0092
	Cd-Se	2	2.567±0.009	0.01368±0.00710	0.9	0.0092
QDs (III)	Cd-S	2.7	2.516±0.005	0.00929±0.00334	0.7	0.0211
	Cd-Se	1.3	2.589±0.005	0.00160±0.00092	0.7	0.0211

Cultural Heritage: SR-XRF Mapping

- Data Format: HDF5 File importable in PyMca
- XRF Elemental mapping, ROI Batch Fit,

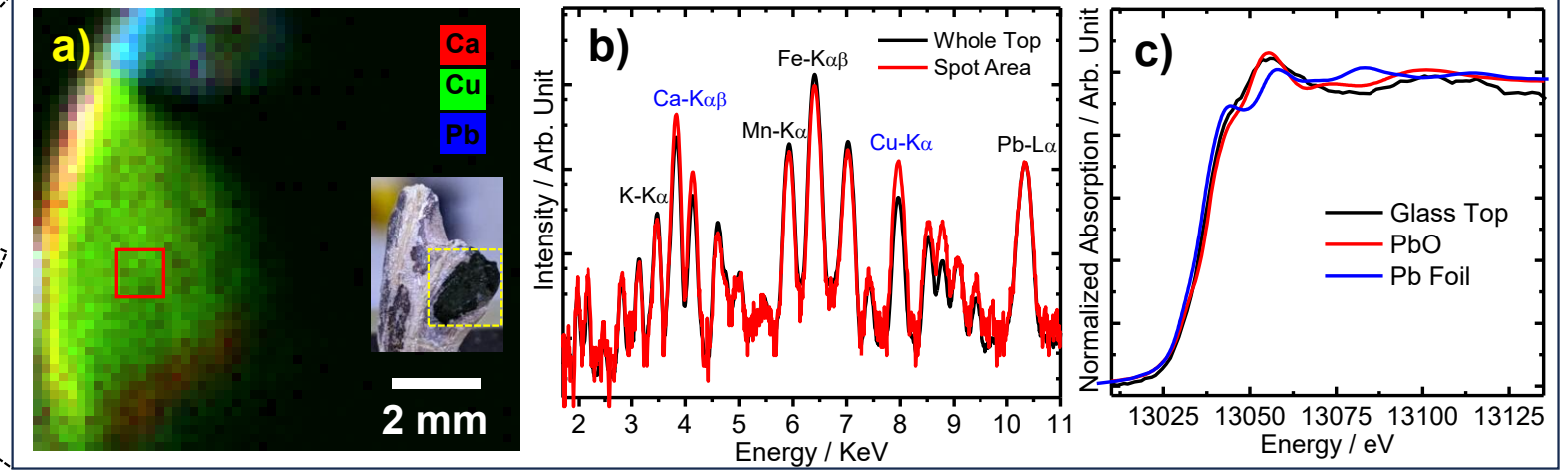

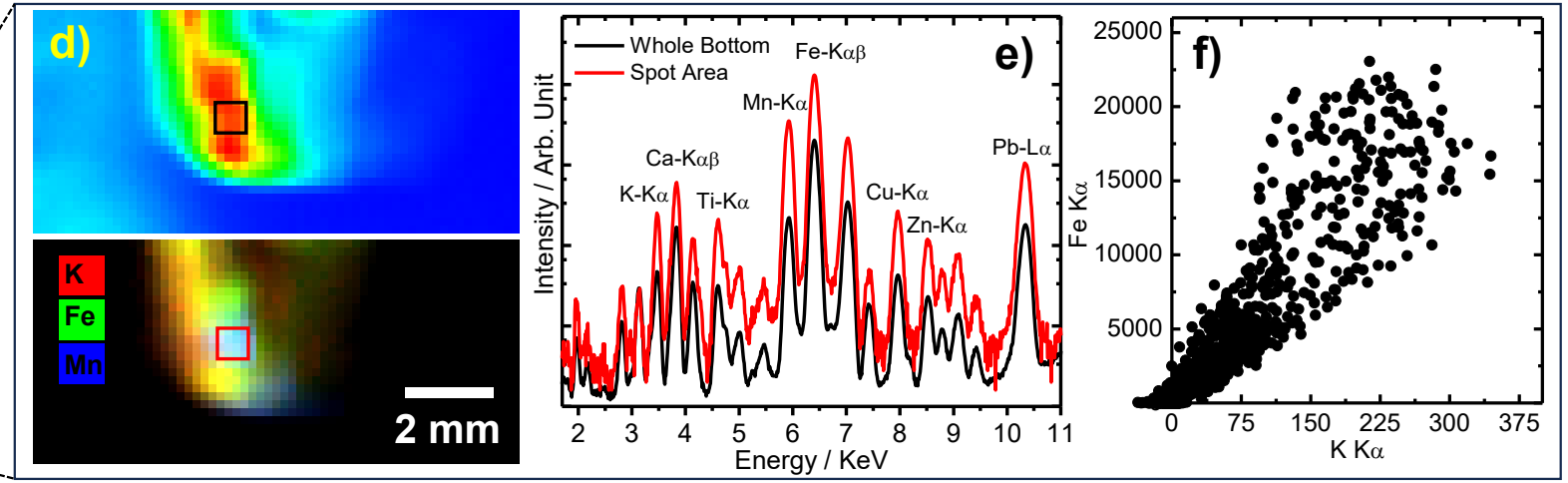

Xray Tomography and XRF mapping of Roman glass sample from Petra, Jordan

Gianluca Iori, Latif U. Khan et al. Non-destructive examination of ancient vitreous materials from Southwest Asia: synchrotron computed tomography at the BEATS beamline of SESAME. *Journal of Cultural Heritage*, 160-168, 2025.

AI-Driven XAS Data Analysis

SESAME

Unlocking Unknown?

New Material

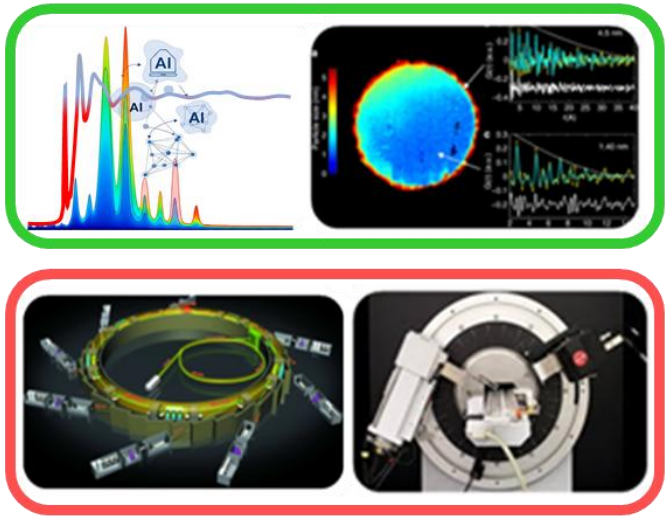

New Structure

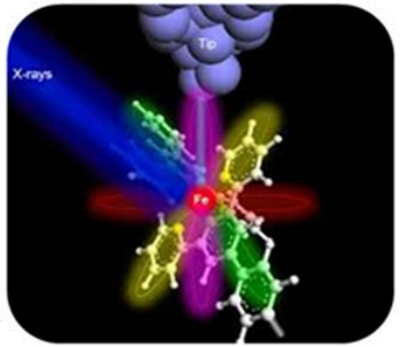

AI is revolutionizing XAFS by transforming complex spectral interpretation into faster, smarter, and more accurate insights.

Need for AI assisted XAFS data analysis

- Accelerates processing of large-scale XAFS datasets
- Enhances accuracy of local structural determination around absorbing atoms
- Though latest generation beamlines produce big data in minimal time, posing inherent challenges for traditional XAS data analysis techniques, however, no available well-developed AI pipeline for real-time XAS prediction.

Machine Learning-Driven XAFS Analysis

Continuous Efforts in Literature on implementing Machine Learning Models in XAFS

- **PyFitIt/FDMNES:** Implementing **neural network** for probing local atomic structure of metal site from XANES
- **EvAX code:** Implementing **evolutionary algorithm** with reverse Monte Carlo modeling for EXAFS data analysis to probe local structure
- **Supervised learning models** in probing nanoparticles' size and structural transformation

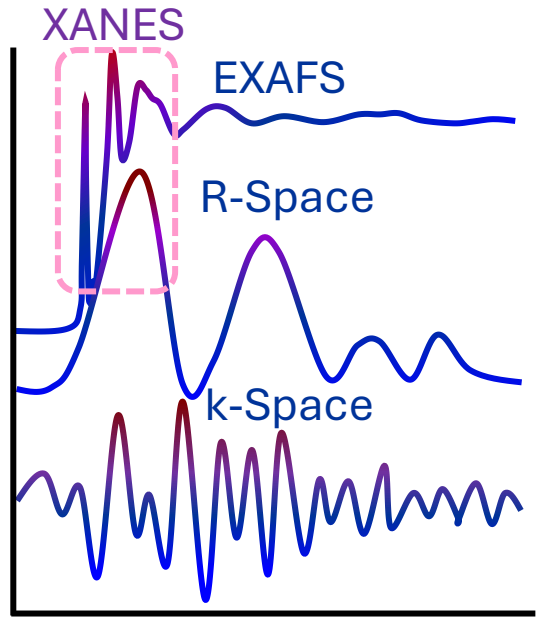

Input Datasets

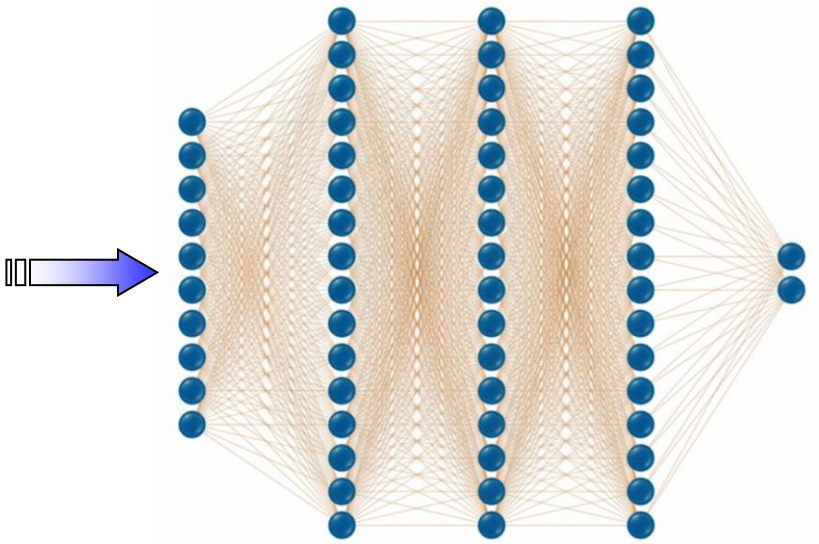

Deep Learning / Neural Network

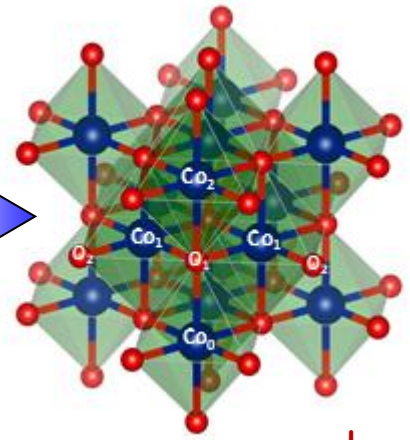

Output

Metal Oxidation State

Coordination geometry / Local 3D structure of metal site

Theoretical XANES Calculation - FDMNES

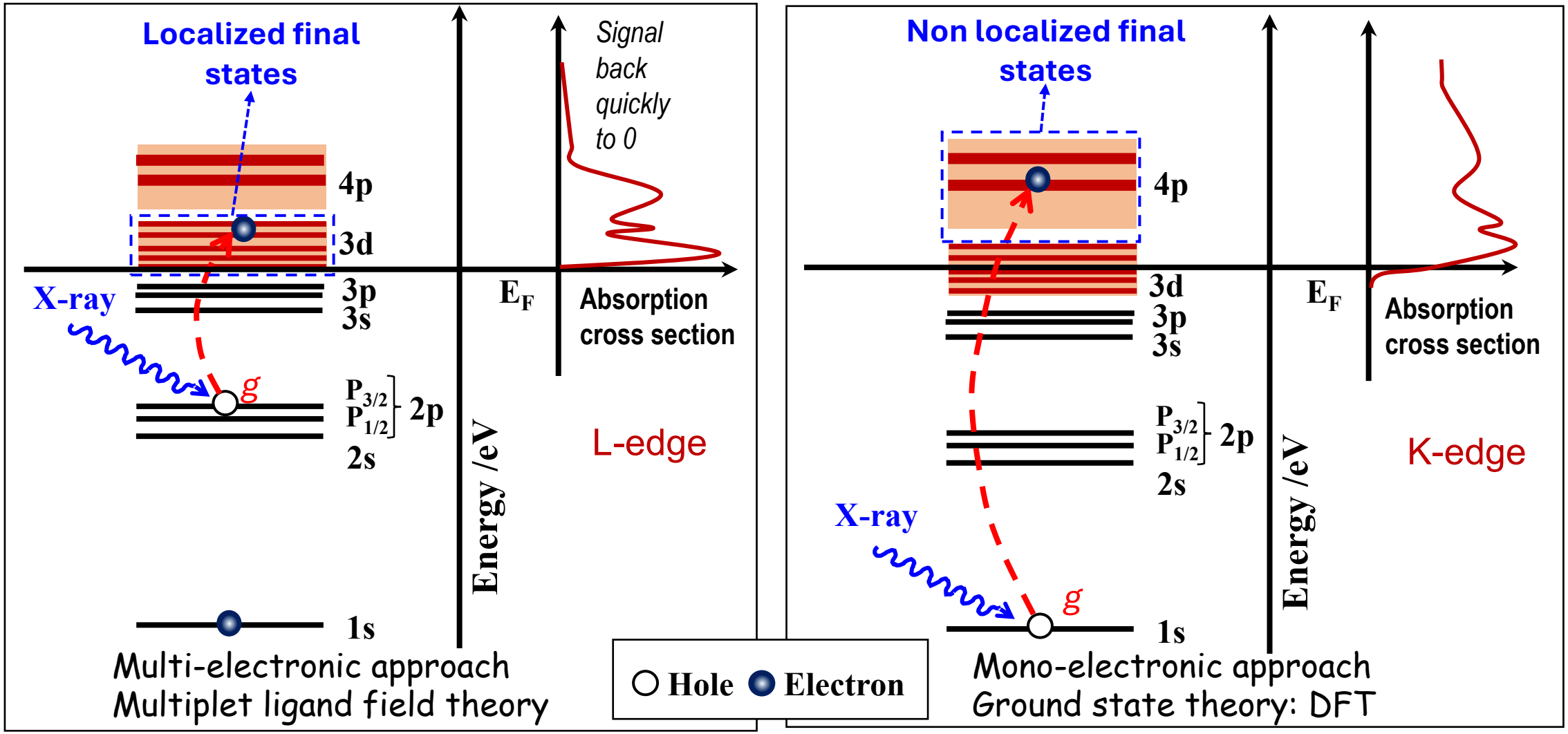

Yves Joly and Stephane Grenier, Theory of X-Ray Absorption Near Edge Structure, *Ch. 4, In book: X-Ray Absorption and X-Ray Emission Spectroscopy,* 2016.

Selection Rules/Electron Transition - FDMNES

SESAME

Electronic Transition Operator $\hat{O}$ is expanded as:

$$\hat{O} = \hat{O}_{E1} + \hat{O}_{E2} + \hat{O}_{E3} + \hat{O}_{M1} + \cdots$$

E1	***E2***	***E3***	***M1***
Electric Dipole	Electric quadrupole	Electric octupole	Magnetic dipole transition
$\Delta\ell = \pm 1$	$\Delta\ell = 0, \pm 2$	$\Delta\ell = \pm 1, \pm 3$	$\Delta\ell = 0$ $\Delta\sigma = 0, \pm 1$

$$\hat{O}_{E1} = \varepsilon.\mathrm{r} \qquad \hat{O}_{E2} = \frac{i}{2}(\varepsilon.\mathrm{r})(\mathrm{k}.\mathrm{r}) \qquad \hat{O}_{E3} = \frac{1}{6}(\varepsilon.\mathrm{r})\,(\mathrm{k}.\mathrm{r})^2$$

$$\hat{O}_{M1} = c_m(\mathrm{k}\times\varepsilon).(\mathrm{L}+2\mathrm{S}) \qquad \text{Where } c_m = \frac{\hbar}{2m(E_f - E_g)}$$

Cross section formula: $\sigma(\omega) = 4\pi^2\,\alpha\hbar\omega \sum_F |\langle f|\hat{O}|g\rangle|^2 \delta(\hbar\omega - E_f + E_g)$

- In X-ray absorption edges, ***E1*** is highly dominant: FDMNES code and PyFitIt consider ***E1*** as default parameter
- ***E2*** typically represents some percentages of ***E1***, and user defined in FDMNES/PyFitIt

PyFitIt Package: Machine Learning

- **PyFitIt**, a machine learning (*i.e.*, implementing neural network) based XANES simulation technique, exploiting the PyFitIt Python library with Python codes in Jupyter notebooks.
- Direct (prediction of a XANES spectrum for a given set of structural parameters) and indirect (prediction of a set of structural parameters for a given XANES spectrum) approaches for the XANES prediction and the corresponding 3D structural refinement.
- FDMNES or FEFF or ADF codes to calculate the *ab initio* theoretical XANES.
- These methods developed for the Big Data or multidimensional data tasks and appropriate to run on the multicore's clusters (local computer very long time).
- 3D structure (XYZ) as input data and sampling points P_1, P_2, . . . , P_N for the training set can be selected by grid and improved Latin hypercube sampling (IHS).

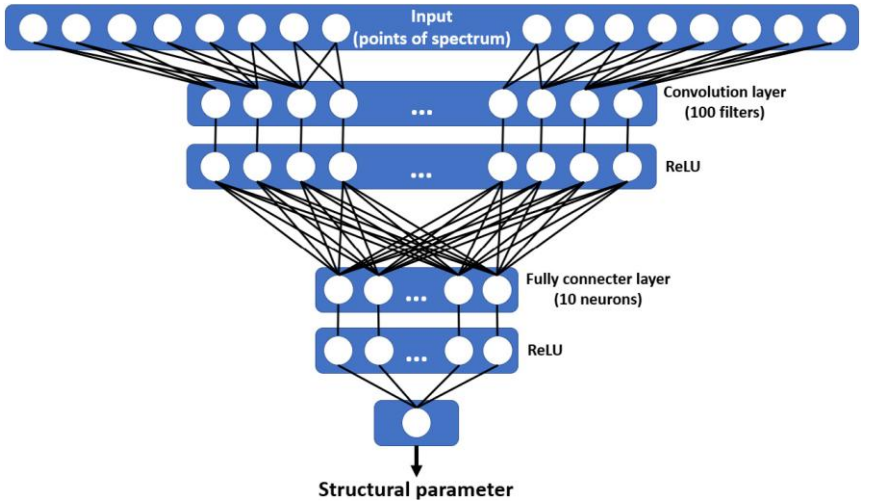

Neural network implemented in PyFitIt

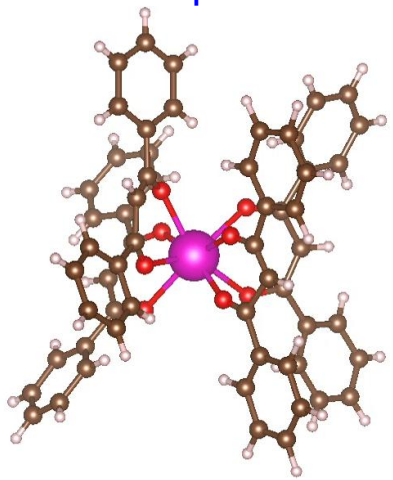

3D Structure

A. Martini, S.A. Guda, A.A. Guda et al. PyFitit: The software for quantitative analysis of XANES spectra using machine-learning algorithm. *Computer Physics Communications* 250 (2020) 107064.

RE^{3+} β-Diketonates: XANES Simulation

- Sm^{3+}, Gd^{3+} and Eu^{3+} β-diketonates
- Fabrication of single-layer organic light-emitting memory devices
- Modern optical quantum memories
- Organic light emitting diodes (OLEDs).
- Gd (III) complex, an excellent T_1 contrast agents in MRI imaging

Samples provided by Prof. Hermi F. Brito, Laboratory of *f*-block elements, Institute of Chemistry University of Sao Paulo Brazil

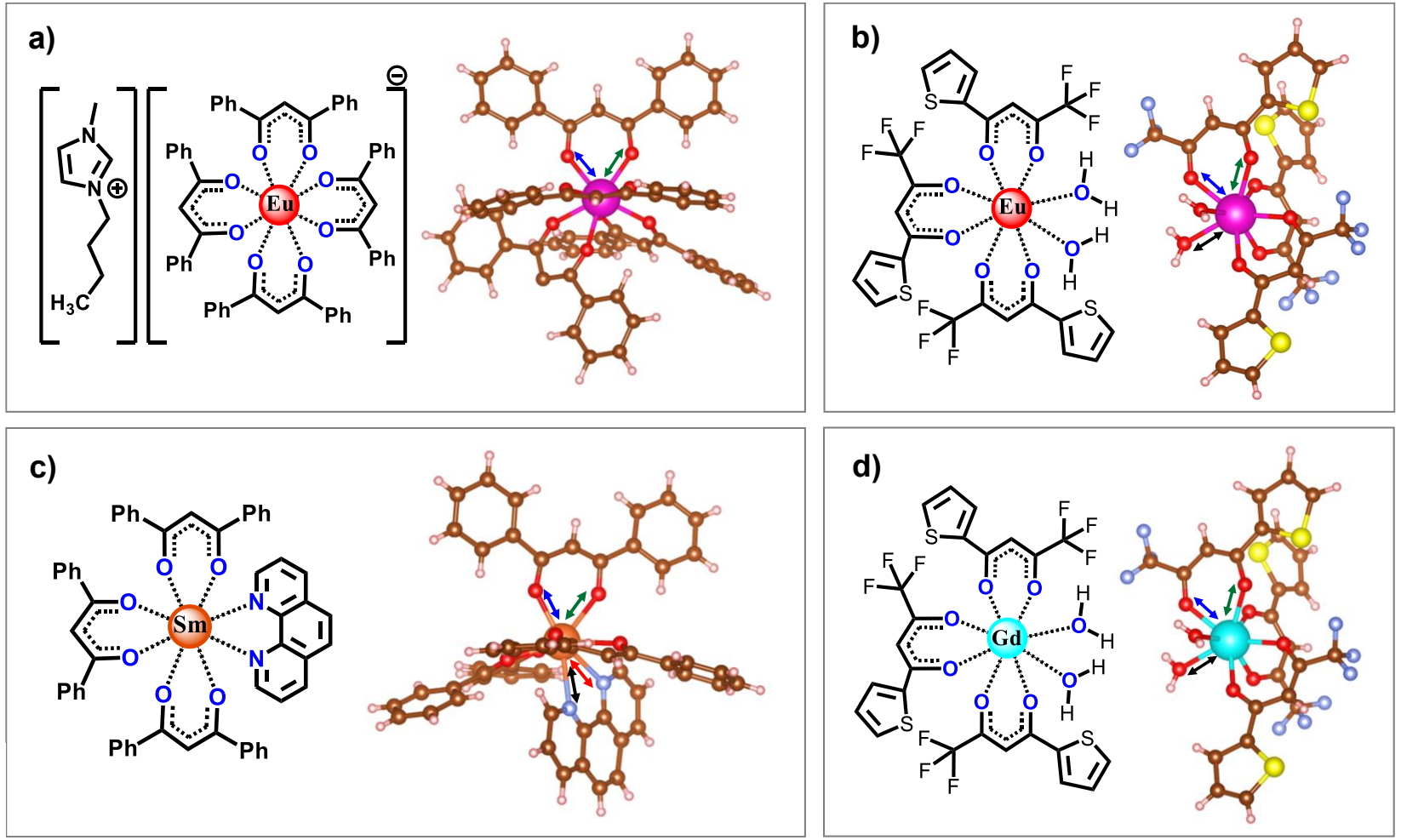

Khan, L. U. et al. Strategy to Probe the Local Atomic Structure of Luminescent Rare Earth Complexes by X-ray Absorption Near-Edge Spectroscopy Simulation Using a Machine Learning-Based PyFitIt Approach. *Inorganic Chemistry (ACS), 62*, 2738–2750, 2023.

Intramolecular Energy Transfer

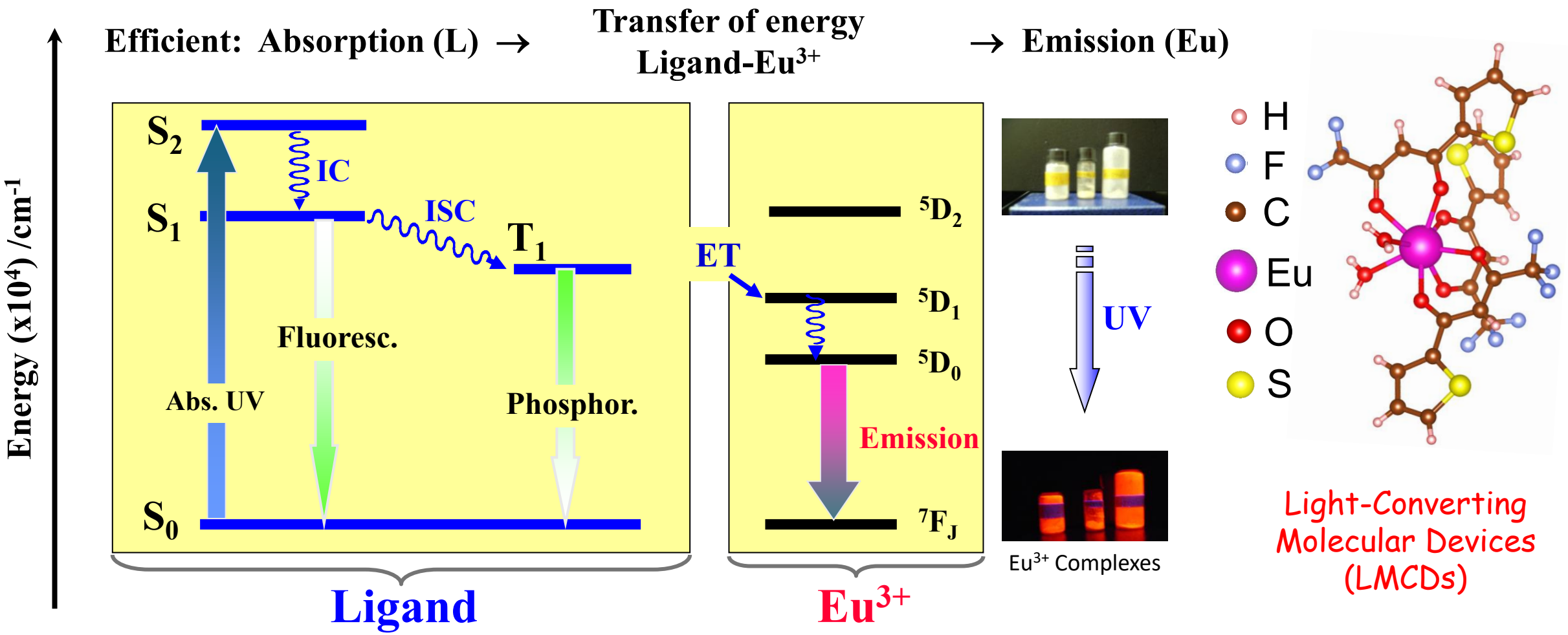

PyFitIt XANES Simulation: Eu^{3+} Complex

SESAME

- PyFitIt, indirect approach to simulate the experimental XANES spectrum of Eu^{3+} tetrakis complex .
- FDMNES code to calculate the *ab initio* theoretical XANES.
- 3D structure (XYZ) with experimental XANES were used as an input data.

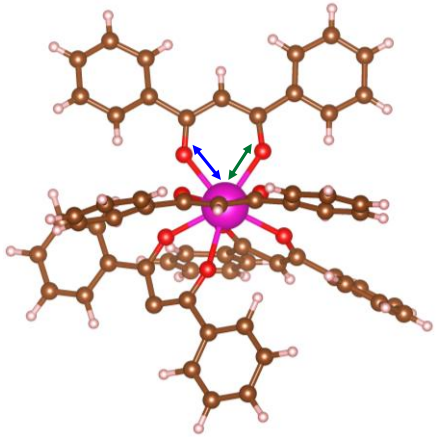

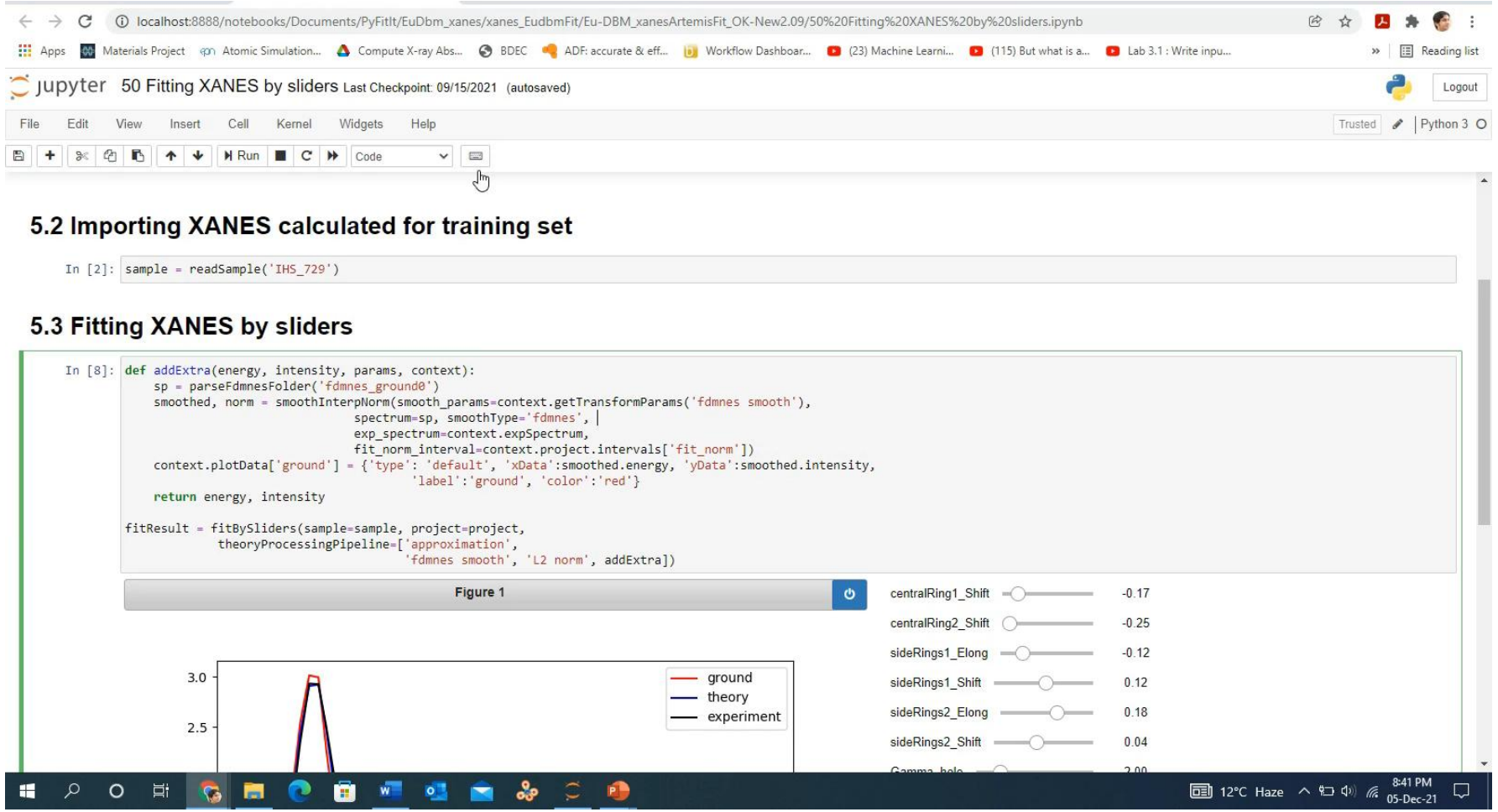

Khan, L. U. et al. Strategy to Probe the Local Atomic Structure of Luminescent Rare Earth Complexes by X-ray Absorption Near-Edge Spectroscopy Simulation Using a Machine Learning-Based PyFitIt Approach. *Inorganic Chemistry (ACS), 62*, 2738–2750, 2023.

Validating PyFitIt Structures via EXAFS Fit

- **EXAFS Fit: Artemis from Demeter**
- $[C_4mim][Eu(dbm)_4]$ complex (left)
- $[Eu(tta)_3(H_2O)_2]$ complex (right)
- The XYZ 3D structures obtained from the PyFitIt XANES simulation were used in EXAFS fit
- feff input files were generated from the corresponding 3D structures in MOLDRAW software

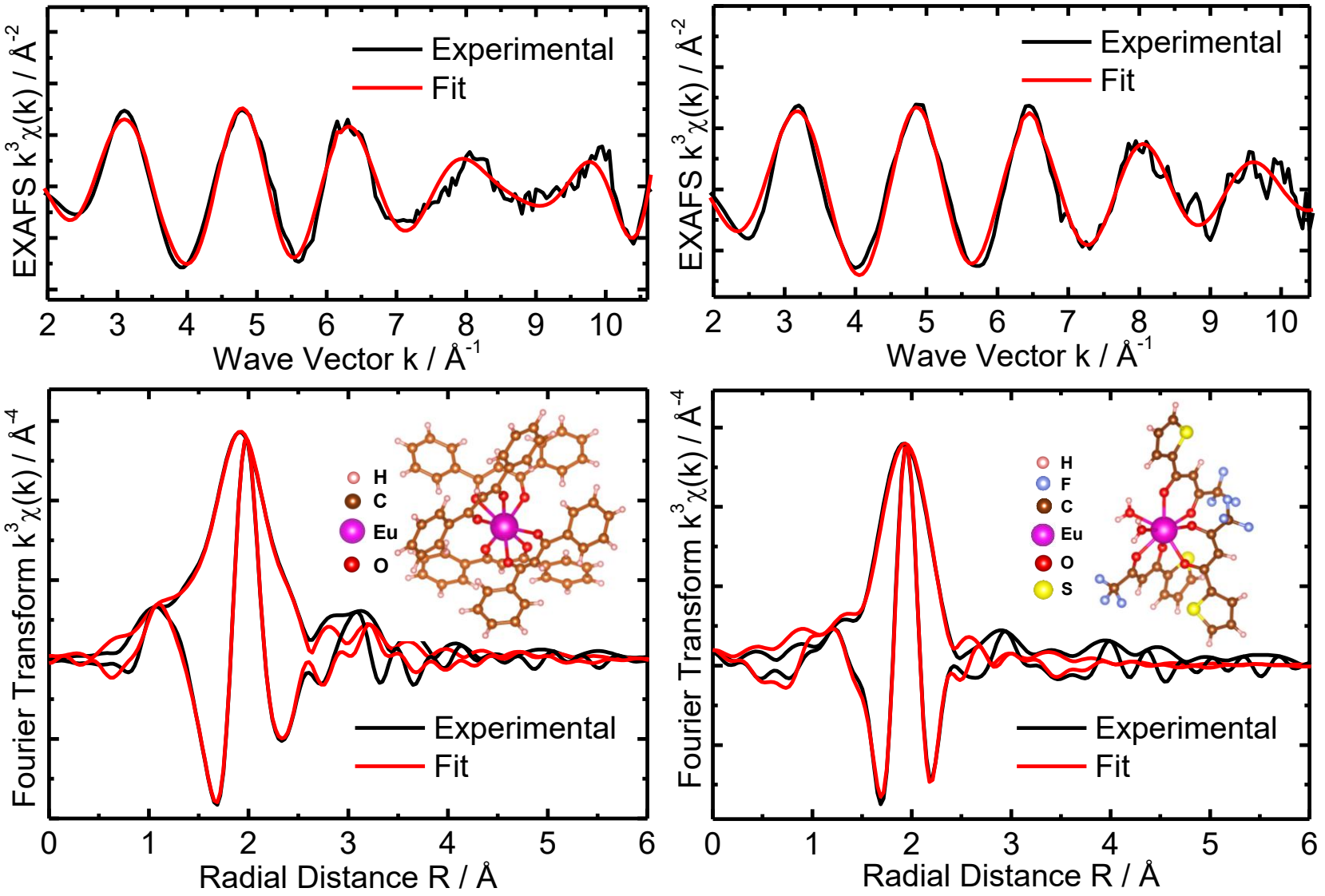

Validating PyFitIt Result *via* Optical Properties

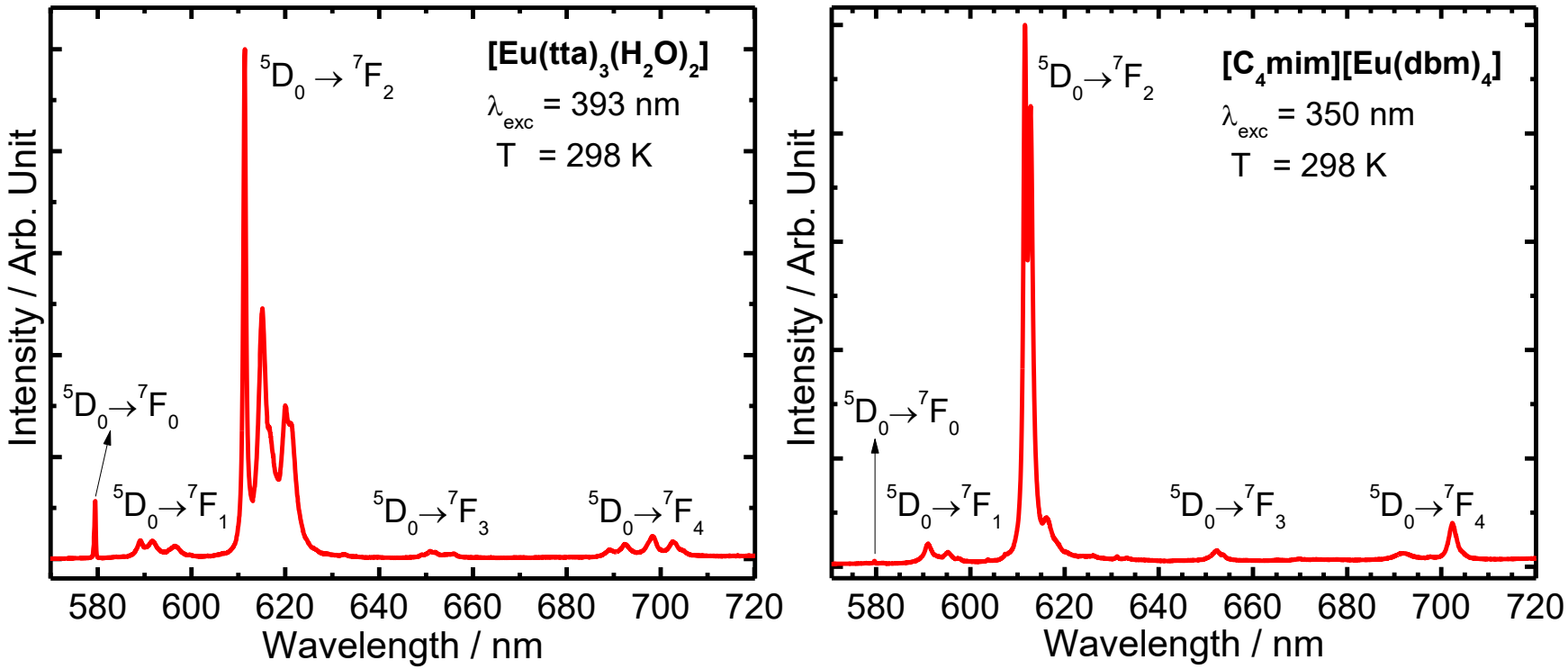

Emission spectra of the $[Eu(tta)_3(H_2O)_2]$ (left) and $[C_4mim][Eu(tta)_4]$ (right) complexes recorded in solid state at 298 K temperature under excitations corresponded to the $S_0 \rightarrow S_n$ transitions of the corresponding organic ligands.

Khan, L. U. et al. Strategy to Probe the Local Atomic Structure of Luminescent Rare Earth Complexes by X-ray Absorption Near-Edge Spectroscopy Simulation Using a Machine Learning-Based PyFitIt Approach. *Inorganic Chemistry (ACS), 62*, 2738–2750, 2023.

4f-4f Intensity Parameters (Ω_λ)

$$A_{0\to J'}(\text{exp.}) = \frac{4e^2\omega_{0\to J'}}{3\hbar c^3(2J+1)}\left[\frac{n(n^2+2)^2}{9}\right]\left\langle {}^5D_0\left\|U^{(\lambda)}\right\|{}^7F_\lambda\right\rangle^2\Omega_\lambda(\text{exp.})$$

Refractive index

Lorentz local field correction (χ)

Reduced element matrix

Experimental and theoretical intensity parameters (Ω_λ, λ = 2 and 4) for the $[Eu(tta)_3(H_2O)_2]$ and $[C_4mim][Eu(tta)_4]$ complexes.

Complex	Ω_2		Ω_4	
	Experimental	PyFitIt	Experimental	PyFitIt
$[C_4mim][Eu(dbm)_4]$	29 ± 1	28.99 ± 0.08	5.8 ± 0.7	5.80 ± 0.14
$[Eu(tta)_3(H_2O)_2]$	32 ± 1	32.00 ± 0.01	6.8 ± 0.8	7.07 ± 0.01

The spontaneous emission coefficients ($A_{0\to J}$) are given by

$$A_{0\to J} = \left(\frac{S_{0\to J}}{S_{0\to 1}}\right)A_{0\to 1}$$

Oscar L. Malta et al. JOYSpectra: A web platform for luminescence of lanthanides. Optical Materials: X 11 (2021) 100080.

EXAFS: Photoelectron Waves

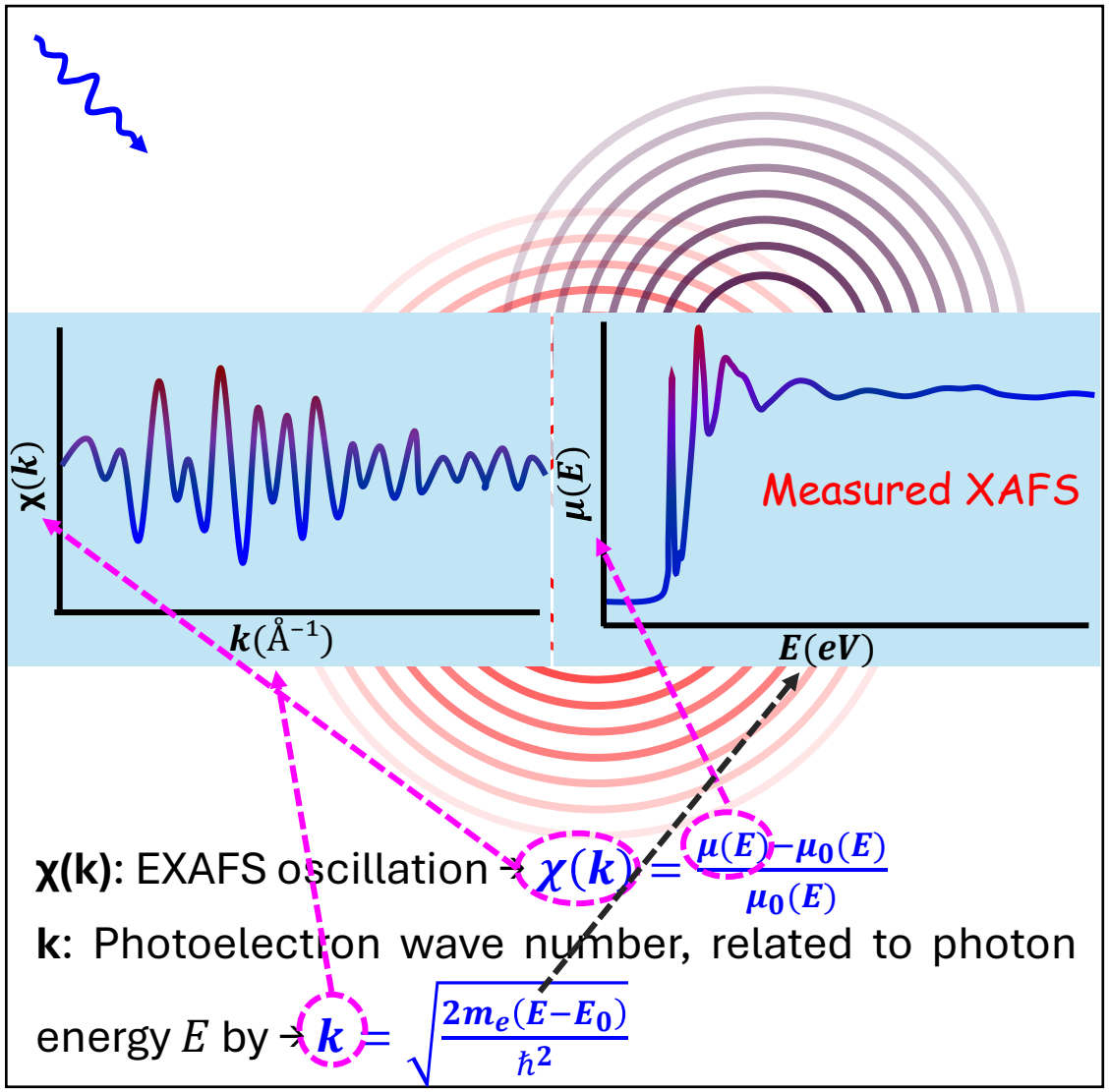

χ(k): EXAFS oscillation → $\chi(k) = \frac{\mu(E) - \mu_0(E)}{\mu_0(E)}$

k: Photoelectron wave number, related to photon energy E by → $k = \sqrt{\frac{2m_e(E-E_0)}{\hbar^2}}$

Scattering (Single/Multiple) of photoelectron in form of waves called stationary waves from the neighboring atoms generate backscattering waves that undergoes interference to generate maximum and minimum of oscillations.

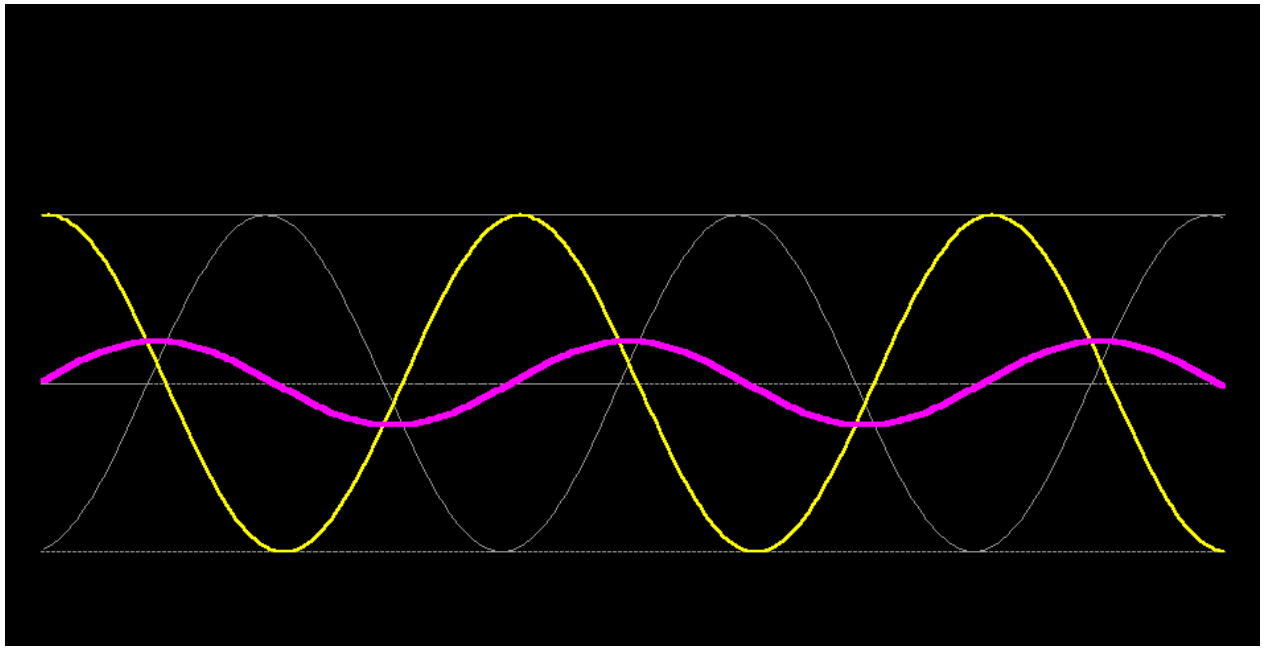

$$\chi(k) = \sum_j S_0^2 \frac{N_j}{kR_j^2} |f_j(k,R_j)| e^{-2R_j/\lambda_j(k)} e^{-2k^2\sigma_j^2} \sin[2kR_j + \phi_j(k)]$$

EXAFS Equation: *ab-initio* χ(k) calculation via FEFF

Machine Learning-Driven XAFS Analysis

Continuous Efforts in Literature on implementing Machine Learning Models in XAFS

- **PyFitIt/FDMNES:** Implementing **neural network** for probing local atomic structure of metal site from XANES
- **EvAX code:** Implementing **evolutionary algorithm** with reverse Monte Carlo modeling for EXAFS data analysis to probe local structure
- **Supervised learning models** in probing nanoparticles' size and structural transformation

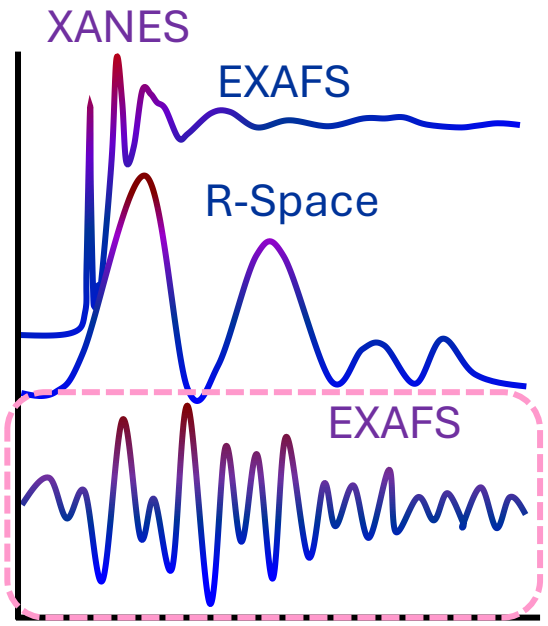

Input Datasets

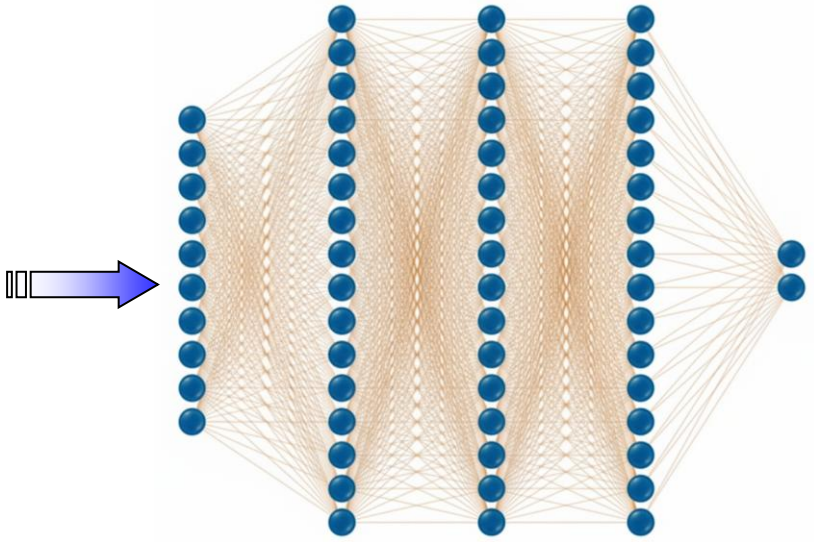

Deep Learning / Neural Network

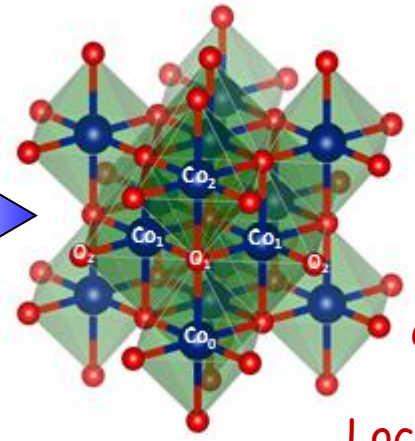

Output

Metal Oxidation State

Coordination geometry / Local 3D structure of metal site

Artificial Neural Network

Artificial neural networks: Inspired by structure and function of human brain, translated to computer.

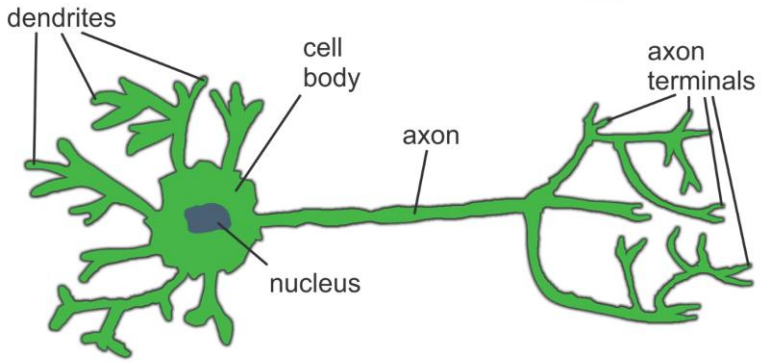

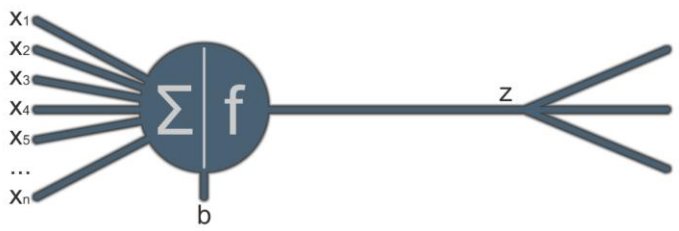

Combining hundreds / thousands (or more) neurons in **neural network**, the interconnectivity produces relationships and results that frequently outperform any other machine learning methods.

Layer sizes: 10, 16, 16, 16, 2

Weights (w): 704
Biases (b): 50
Params: 704

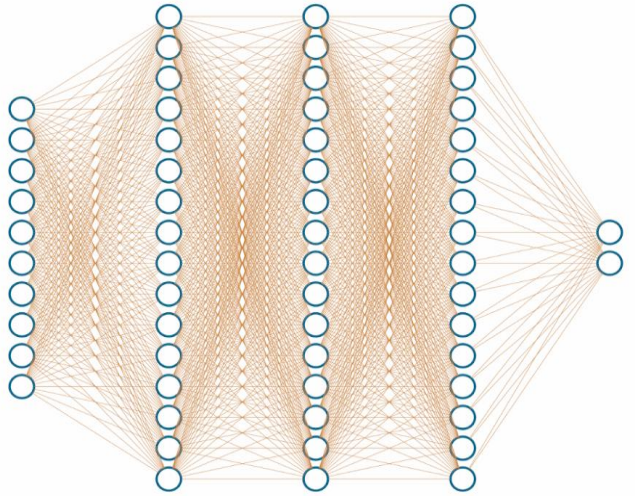

Neural network with 3 hidden layers of 16 neurons in each

TensorFlow is an open-source machine learning framework developed by Google. It provides excellent support for implementing Convolutional Neural Network (CNN) or Physics-Informed Neural Networks (PINNs), which can be utilized to train on specific spectral datasets.

Physics Informed Neural Network (PINN)

SESAME

PINNs in EXAFS data prediction

Aspect	Physics-Informed Neural Networks (PINNs)	Conventional Deep Learning CNNs
Data Requirement	Require relatively small datasets due to embedded physics constraints	Require large labeled datasets to achieve good performance
Physical Consistency	Predictions strictly obey governing physics laws (e.g., EXAFS equation, scattering theory etc.)	May produce non-physical outputs that violate known scientific relationships
Generalization	High generalization to unseen spectra of materials' EXAFS	Poor extrapolation to unseen spectra
Interpretability	Provides meaningful parameters and insights in local structure prediction (e.g., coordination numbers, bond distances etc.)	Limited physical interpretability
Noise Robustness	Handles noisy experimental data effectively	Sensitive to noise and performance degrades with noisy data
Training Objective	Combines data loss and physics-informed loss	Optimizes only data loss
Computational Efficiency	Slightly higher training cost due to PDE constraints, but yields more reliable solutions	Faster training but may need more data and post-corrections
Model Output Quality	Generates smooth/physically valid **EXAFS data [χ(k)/χ(R)]**	May produce unrealistic EXAFS oscillations or artifacts in spectra

EXAFS Prediction: Model Training

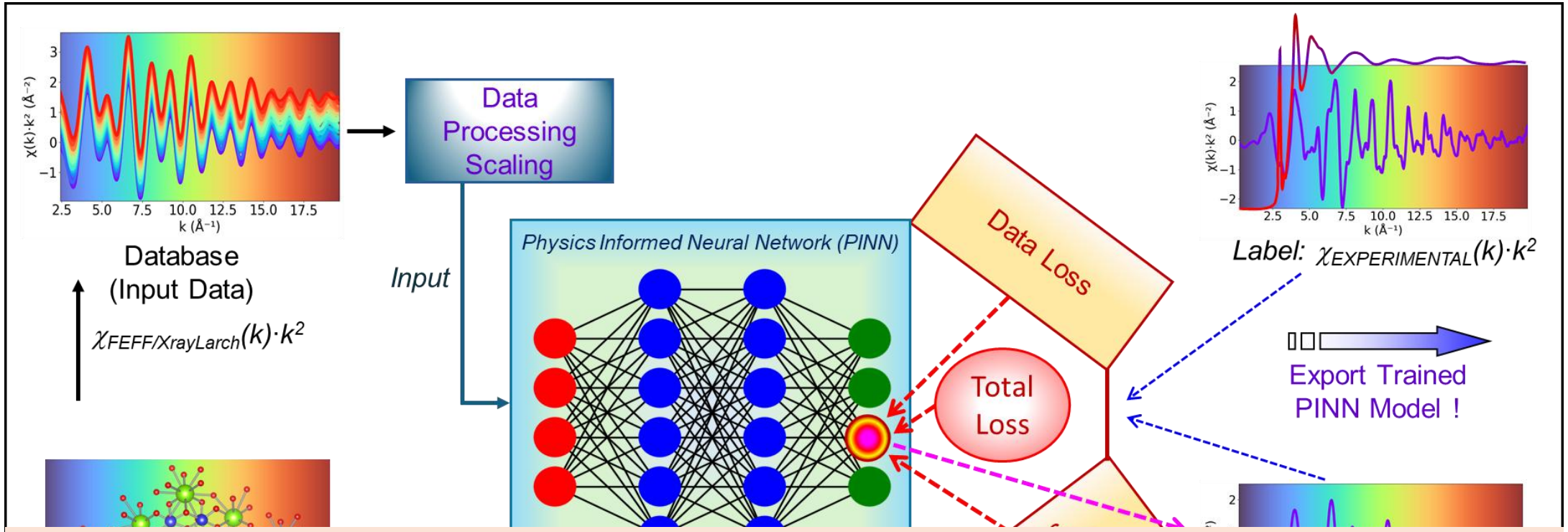

In context of XAFS spectral modeling (**EXAFS χ(k) or χ(R)** analysis), $\mathcal{L}_{data}$ guides the neural network to reproduce experimental spectra accurately, while $\mathcal{L}_{PI}$ ensures that the learned solution remains consistent with the underlying EXAFS theory (FEFF/XrayLarch). This hybrid loss enables the model to generalize effectively, even in regions with noisy data.

https://github.com/khanlatif001/PINNmodel_EXAFS-Prediction

Model Training & EXAFS Prediction

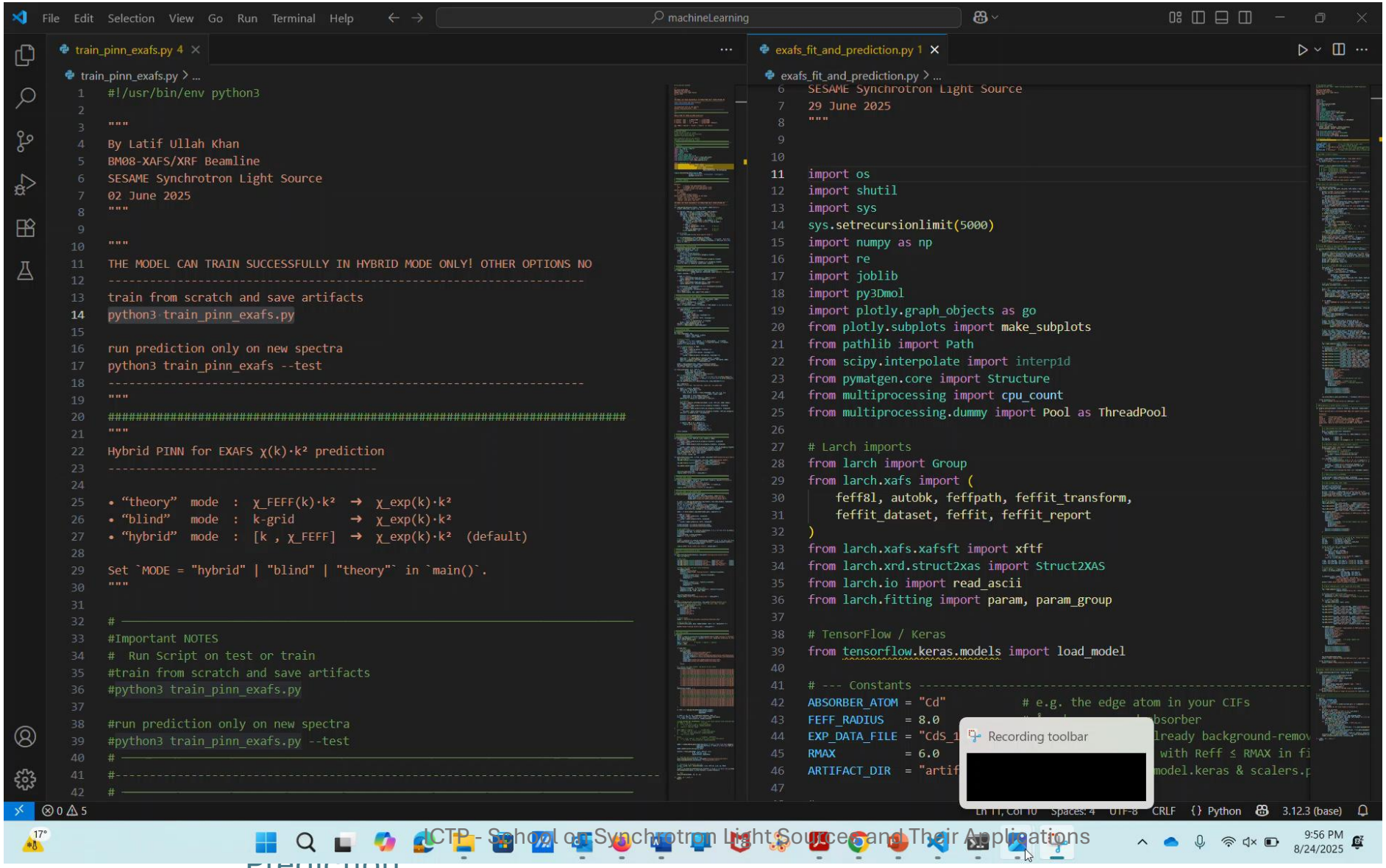

EXAFS Prediction Result

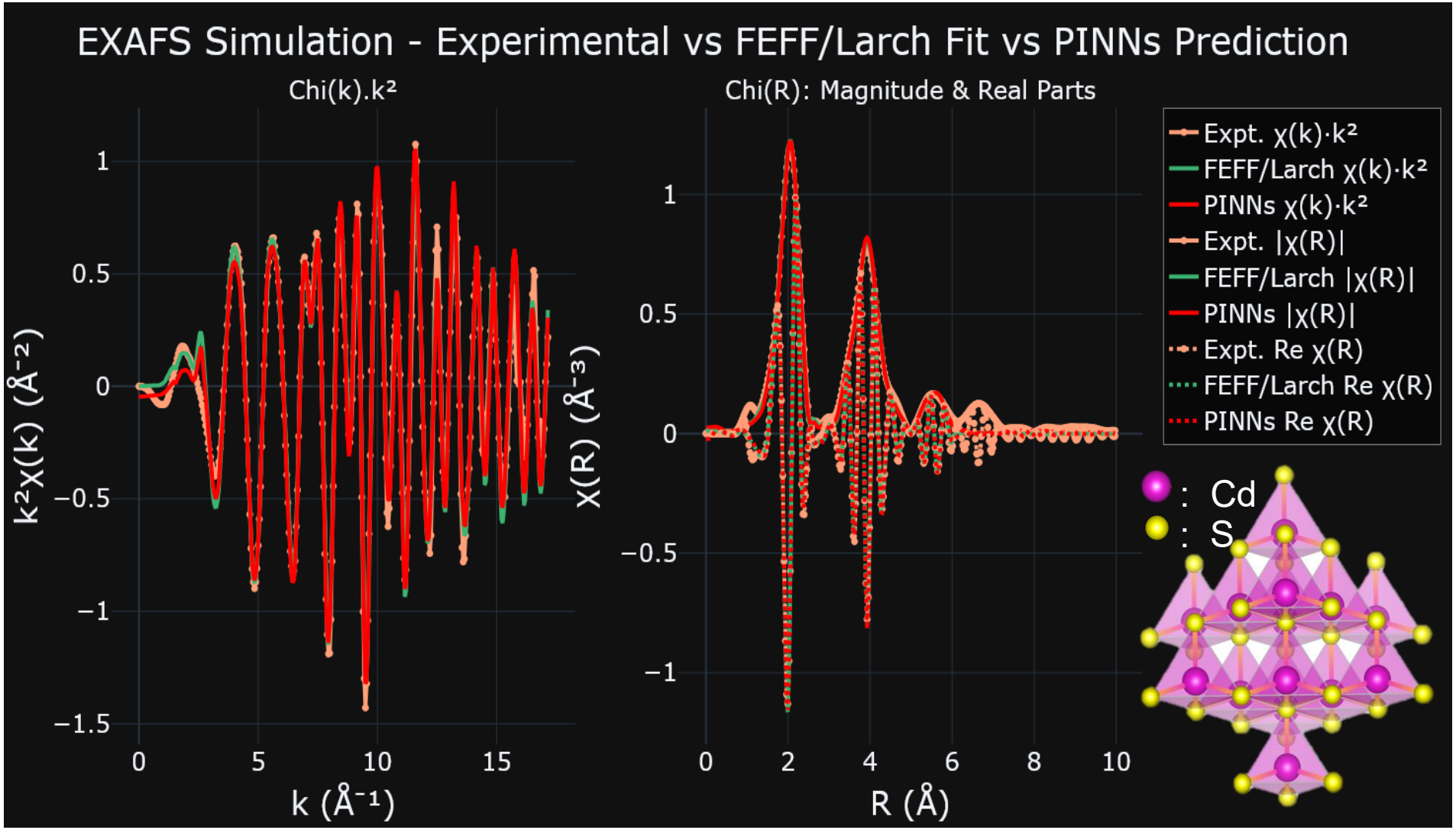

https://github.com/khanlatif001/PINNmodel_EXAFS-Prediction

XEOL/XAS Publications 2025

SESAME

1) Cardenas Rodriguez, C.Y.; Polozhentsev, O.; Alamoush, M.; Shukla, N.; Mukhanova, E.A.; Soldatov, A.V. Phase transition and size-tunable synthesis of Tb^{3+}/Ce^{3+} co-doped hexagonal GdF_3 nanoparticles: Structural characterization, optical, scintillation and magnetic properties, **Journal of Alloys and Compounds**, Vol. 1032, pp. 181102, 2025.

2) Gul I.; Khan, Z.U.; Galani, S.; Huda, S.; Khan, L.U.; Juwhari, H.K.; Hyder, A.; Brito, H.F.; Zaheer, M.; Khan, M.A. Gd3+ and Sm3+ ions modulated visible-light-emitting ZnSe:Mn^{2+} nanocrystals for detection of Pb^{2+} and Hg^{2+}. **ACS Applied Optical Materials**, Vol. 9, pp. 2067–2077, 2025.

3) Gul I.; Khan, Z.U.; Khan, M.A.; Cabrera-Pasca, G.A.; AlZubi, R.I.; Figueroa, S.J.A.; Brito, H.F.; Khan, L.U. Ln^{3+}-ion-mediated enhancement in UV/X-ray-induced optical emission from Mn^{2+}-doped ZnSe nanocrystals. **Nanoscale (RSC)**, 2025. https://doi.org/10.1039/D5NR01263E

4) AlZubi, R.I.; Khan, Z.U.; Aldrabee, A.; Khan, L.U. Synchrotron Radiation X-ray Excited Optical Luminescence Probing of Green Emission from Gd_2O_2S:Tb/PVP Scintillator. In: Jakka, S.K., Krishnapuram, P., Graça, M.P.F. (eds) Selected Articles of the 2nd International Conference on Spectroscopy in Materials Science. ICOSIMS-2024. **Springer Proceedings in Physics**, vol 422, 2025, Springer, Singapore. https://doi.org/10.1007/978-981-96-4035-5_3

5) Khan, L.U.; AlZubi, R.; Juwhari, H. K.; Mousa, Y.A.; Khan, Z.U.; Figueroa, S.J.A.; Hans, P. Advanced Probing of Eu^{2+}/Eu^{3+} Photoemitter sites in $BaAl_2O_4$:Eu scintillators by Synchrotron Radiation X-ray Excited Optical Luminescence Probe. **Optical Materials (Elsevier)**, 2025, https://doi.org/10.1016/j.optmat.2025.116937

6) Khan, L.U.; Khan, Z.U. AlZubi, R.; Umer, M. A.; Juwhari, H. K.; Harfouche, M. and Brito, H.F. Tracking coordination environment and optoelectronic structure of Eu^{3+} and Sm^{3+} sites via x-ray absorption spectroscopy and x-ray excited optical luminescence. **Materials Today: Proceedings**, March 2024. https://doi.org/10.1016/j.matpr.2024.03.028

Acknowledgments

Dr. Santiago Figueroa
XAFS - QUATI BL
(SIRIUS LNLS)

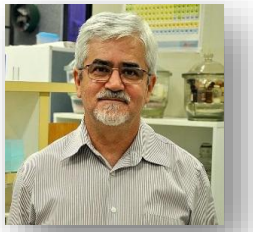

Prof. Hermi F Brito
Electr. Spectroscopy
(IQ-USP)

Prof. Oscar Malta
Theor. Electr. Spectroscopy
(DQF-UFPE)

Prof. Marcelo Knobel
Nanomagnetism Physics IFGW
(ex-Rector -UNICAMP)

Prof. Hassan K. Juwhari
Ln. Spectroscopy Physics
(University of Jordan)

Dr. Vronica Teixeira
XEOL - Carnauba BL
(SIRIUS LNLS)

Prof. Magnus
Immune Physiopathology
(ICB-USP)

Prof. Diego Muraca
Nanomagnetism/Microscopy
(IFGW-UNICAMP)

Prof. Kleber
Magnetism Physics
(IFGW-UNICAMP)

Prof. Khaled Badoor
Theoretical Physics
(University of Jordan)

Dr. Carlos Pérez
XRF - Carnauba BL
(SIRIUS LNLS)

Dr. Naila Jabeen
Catalysis Nanotecnology
(NCP Islamabad)

Dr. Zahid Khan
Nanobiotechnology
(RCGI-USP)

Dr. Muhammad Usman
(NCP Islamabad)

Dr. Ruba Alzubi
(JAEC Jordan)

SESAME

Thanks